Post-Stroke Administration of L-4F Promotes Neurovascular and White Matter Remodeling in Type-2 Diabetic Stroke Mice

Min Zhou [1†], Rongwen Li [1], Poornima Venkat [1], Yu Qian [1†], Michael Chopp [1,2], Alex Zacharek [1], Julie Landschoot-Ward [1], Brianna Powell [1], Quan Jiang [1,2] and Xu Cui [1*]*

[1] Department of Neurology, Henry Ford Hospital, Detroit, MI, United States, [2] Department of Physics, Oakland University, Rochester, MI, United States

Patients with type 2 diabetes mellitus (T2DM) exhibit a distinct and high risk of ischemic stroke with worse post-stroke neurovascular and white matter (WM) prognosis than the non-diabetic population. In the central nervous system, the ATP-binding cassette transporter member A 1 (ABCA1), a reverse cholesterol transporter that efflux cellular cholesterol, plays an important role in high-density lipoprotein (HDL) biogenesis and in maintaining neurovascular stability and WM integrity. Our previous study shows that L-4F, an economical apolipoprotein A member I (ApoA-I) mimetic peptide, has neuroprotective effects *via* alleviating neurovascular and WM impairments in the brain of db/db-T2DM stroke mice. To further investigate whether L-4F has neurorestorative benefits in the ischemic brain after stroke in T2DM and elucidate the underlying molecular mechanisms, we subjected middle-aged, brain-ABCA1 deficient (ABCA1$^{-B/-B}$), and ABCA1-floxed (ABCA1$^{fl/fl}$) T2DM control mice to distal middle cerebral artery occlusion. L-4F (16 mg/kg, subcutaneous) treatment was initiated 24 h after stroke and administered once daily for 21 days. Treatment of T2DM-stroke with L-4F improved neurological functional outcome, and decreased hemorrhage, mortality, and BBB leakage identified by decreased albumin infiltration and increased tight-junction and astrocyte end-feet densities, increased cerebral arteriole diameter and smooth muscle cell number, and increased WM density and oligodendrogenesis in the ischemic brain in both ABCA1$^{-B/-B}$ and ABCA1$^{fl/fl}$ T2DM-stroke mice compared with vehicle-control mice, respectively ($p < 0.05$, $n = 9$ or 21/group). The L-4F treatment reduced macrophage infiltration and neuroinflammation identified by decreases in ED-1, monocyte chemoattractant protein-1 (MCP-1), and toll-like receptor 4 (TLR4) expression, and increases in anti-inflammatory factor Insulin-like growth factor 1 (IGF-1) and its receptor IGF-1 receptor β (IGF-1Rβ) in the ischemic brain ($p < 0.05$, $n = 6$/group). These results suggest that post-stroke administration of L-4F may provide a restorative strategy for T2DM-stroke by promoting neurovascular and WM remodeling. Reducing neuroinflammation in the injured brain may contribute at least partially to the restorative effects of L-4F independent of the ABCA1 signaling pathway.

Keywords: diabetes, stroke, blood–brain barrier (BBB), white matter (WM), ABCA1, HDL, neuroinflammation

INTRODUCTION

Type-2 diabetes (T2DM) constitutes ∼90% of all diabetic patients and is a major risk factor for ischemic and hemorrhagic stroke. Epidemiological investigation in both younger (15–49 years) [1] and elderly (>65 years) [2] diabetic patients show a 10 years cumulative recurrent ischemic stroke rate of 29.7% for T2DM, and 12.0% for non-diabetic patients in the 15–49 age group [1], and 4.26% of stroke events and 1.79% of death rates during 6 years of follow-up for >65 age group. Moreover, diabetic-stroke patients exhibit a high level of neuroinflammation, worse neurovascular and white matter (WM) injury with severe and long-lasting neurological deficits compared with non-diabetic stroke patients [1–6]. Neuroinflammation is involved in the onset and progression of stroke which is triggered by the infiltration of blood macrophages (M1 macrophage) and the activation of glial cells (microglia and astrocytes) which then released proinflammatory cytokines/factors. These inflammatory mediators not only lead to neurotoxicity and neuronal dysfunction and also induce blood–brain barrier (BBB) disruption and leakage. BBB damage allows the trafficking of immune cells and/or plasma proteins into the brain parenchyma which amplifies neuroinflammation and exacerbates neurovascular and WM injury [7]. Therefore, there is a compelling need to develop therapeutic strategies for T2DM-stroke patients and elucidate the underlying molecular biological mechanisms.

After adjusting for all possible covariables, blood levels of low-density lipoprotein (LDL) cholesterol show a significant association with increased risk of stroke and mortality [2, 8]. However, high-density lipoprotein (HDL) and HDL-increasing agents, such as Niacin, GW3965, T090317, etc., have demonstrated anti-neuroinflammation capabilities [9–14] and protection of brain vasculature and WM after stroke in preclinical studies [15–20]. In T2DM patients, levels of both HDL and apolipoproteins and their functions such as the antioxidative capacity are impaired, which contribute to neurovascular and WM damage after stroke [8–12, 21–25].

In humans, the circulating blood contains only about 40% of the total amount of HDL, and most of the HDL in the central nervous system (CNS) is synthesized *in situ* mainly by the ATP-binding cassette transporter member A 1 (ABCA1), a reverse cholesterol transporter that efflux cellular cholesterol [26, 27]. ABCA1 not only plays a key role in HDL biogenesis and in maintaining brain cholesterol metabolism, but it also exerts highly anti-atherogenic effects and has remarkable anti-inflammatory properties [28–33]. We have previously demonstrated that deficiency of ABCA1 in the brain induces worse neurological functional deficits after stroke, increases BBB leakage and aggravates OL loss and WM injury [17, 34–36]. The Apolipoprotein A-I (ApoA-I) mimetic peptide, 4F (D-4F, synthesized from D-amino acids, and L-4F, synthesized from L-amino acids) increases cholesterol efflux [37–43] and has anti-inflammatory effects [44–46]. In our previous study, we have shown that treatment of stroke in type 1 diabetes mellitus (T1DM) rats with D-4F or db/db-T2DM stroke mice treated with L-4F significantly decreases neurovascular and WM damage

and improves neurological function in the early stage (4–7 days) after stroke [45, 46]. However, whether L-4F is capable of crossing the BBB and whether long-term post-stroke treatment with L-4F promotes neurovascular and WM remodeling and improves recovery of neurological function in T2DM, and whether ABCA1 mediates L-4F-induced neurorestoration have not been studied. Therefore, in this study, we employ middle-aged, brain-ABCA1 deficient (ABCA1$^{-B/-B}$) and ABCA1-floxed (ABCA1$^{fl/fl}$) control mice that were induced with T2DM and subjected to stroke, to test whether L-4F treatment initiated at 24 h after onset of ischemic stroke enhances neurological recovery. We also test if L-4F treatment improves vascular and WM rewiring in T2DM stroke and whether L-4F decreases inflammation *via* ABCA1 dependent signaling pathway. We demonstrate that L-4F can pass through the BBB and has neurorestorative capabilities in promoting neurovascular and WM remodeling, and oligodendrogenesis in the ischemic brain of T2DM-stroke mice. Our data also indicate that reducing neuroinflammation in the injured brain may contribute at least partially to the neurorestorative effects of L-4F independent of the ABCA1 signaling pathway.

MATERIALS AND METHODS

T2DM Induction

To investigate whether the ABCA1 signaling pathway mediates L-4F-induced neurorestorative in T2DM-stroke mice, ABCA1$^{-B/-B}$ and ABCA1$^{fl/fl}$ mice were employed. The original breeders were provided by Dr. Michael Hayden from the University of British Columbia, Canada. All mice used in this study were self-bred in the Bioresources of Henry Ford Health System, and all procedures were approved by the Institutional Animal Care and Use Committee of Henry Ford Health System (Code No. 1289, Approval Date 04/05, 2021). The litters were heterozygous and the ABCA1$^{-B/-B}$ or ABCA1$^{fl/fl}$ phenotype was identified with genotyping assay [29, 47]. While studying the effects of L-4F in both males and females is critical from a translational point of view, in this study, to exclude the effects of estrogen in females and in order to compare results with our previous studies, only male ABCA1$^{-B/-B}$ and ABCA1$^{fl/fl}$ mice (13-month-old, total 115 mice) were employed. These mice were induced with T2DM using a combination of a high-fat diet (HFD, 60% calories from fat, Research Diets, USA) and a low dose of streptozotocin (STZ, ALX-380-010-G001, Enzo Life Science, USA) injection [48–52]. Briefly, 10-months-old mice were fed an HFD for 2 months. Then, mice were fasted for 6 h and administered STZ on two consecutive days (75 mg/kg, i.p. as first dose and 50 mg/kg, i.p as the second dose). Mice were continued on an HFD for one more month. Bodyweight and fasting blood glucose levels were measured, and mice with glucose >250 mg/dl were considered as T2DM and included in the study.

Stroke Model and Treatment

T2DM mice were subjected to permanent distal right middle cerebral artery occlusion (dMCAo) surgery, as described previously [31]. At 24 h after dMCAo, mice were randomly

divided into 4 groups: 1. ABCA1$^{fl/fl}$ control; 2. ABCA1$^{fl/fl}$ + L-4F; 3. ABCA1$^{-B/-B}$ control; 4. ABCA1$^{-B/-B}$ + L-4F. Mice were administered 16 mg/kg L-4F (BioMatik, Cambridge, ON, Canada) or saline subcutaneously starting at 24 h after dMCAo and once daily for 21 days. The dose of L-4F employed in this study is the same as the optimal dose of D-4F which was employed in our previous study (18). The treatment route using subcutaneous administration of saline or L-4F in this study is consistent with the treatment route employed in our previous publication (46). Mice were sacrificed at 21 days after dMCAo. A total of 86 mice were included excluding mice that died at early time points after stroke and mice with lesion volume < 6%. To record mortality, all the animals were counted daily and the percentage of dead animals in each group was counted within the 21 days after dMCAo.

Behavioral Testing

To evaluate neurological function after stroke, all animals were subject to an adhesive removal test and left foot-fault test before dMCAo (baseline) and on days 1, 3, 7, 14, and 21 after dMCAo, as described previously (19, 53). Experimental groups and treatments were double-blinded to the investigators who performed testing and analyzed data.

Blood Biochemistry Measurement

To test blood biochemistry, animals were fasted for 6 h, and blood was collected from a tail vein before treatment on day 1 after dMCAo as the baseline measurement and before sacrifice on day 21 after treatment. Blood glucose levels were measured using glucose test strips and a glucose analyzer (Accu-Chek Compact System; Roche Diagnostics, Basel, Switzerland). Blood levels of HDL, total cholesterol (T-CH), and triglyceride were measured using a CardioChek Plus analyzer 2,700 (Polymer Technology System Inc., Indianapolis, IN) and test strips, following the manufacturer's instructions. Each sample was tested in triplicate and the data are presented as mg/dl.

Cerebral Hemorrhagic Transformation and Lesion Volume Measurement

Briefly, brains were immersion fixed in 4% paraformaldehyde, paraffin-embedded, and then cut into seven (1 mm thick) coronal blocks. A series of 6 μm thick sections were prepared and stained with hematoxylin and eosin (HE), and hemorrhagic transformation was identified by blood cell infiltration in the cerebral ischemic brain and the percentage of hemorrhagic transformation volume was calculated. For lesion volume measurement, the percentage of the indirect lesion volume was calculated, in which the intact area of the ipsilateral hemisphere was subtracted from the area of the contralateral hemisphere, with a micro-computer imaging device (MCID) imaging analysis system (Imaging Research, ST. Catharines, ON, Canada) (54).

Histochemical and Immunohistological Staining

For histochemical/immunostaining, a standard paraffin block was obtained from the center of the lesion (bregma −1 mm to + 1 mm). A series of 6-μm thick sections were cut from

the block. Histochemical-staining for Bielshowsky silver (BS, an axon marker) and Luxol fast blue (LFB, a myelin marker), and histoimmuno-staining for antibodies against albumin (BBB leakage marker, 1:500; ab53435, Abcam), Occludin (a marker of tight junction, OC-3F10, 1:100, Fisher), Aquaporin-4 (AQP4, a protein expressed in astrocytic end-feet as another marker of BBB, 1:1,500; ab3594, EMD Millipore), von Willebrand Factor (vWF, a vessel marker, 1:400; A0082, Dako), α-smooth muscle actin (αSMA, a smooth muscle cell-SMC marker, 1:800, Dako), SMI31 (a marker of phosphorylated-neurofilament, 1:1,000, Covance), adenomatous polyposis coli [APC, a marker of mature oligodendrocytes-OLs (55), Ab-1, OP44, 1:100; Calbiochem], and platelet-derived growth factor receptor alpha (PDGFRα, a marker of oligodendrocyte progenitor cells-OPCs, C-20, SC-338, 1:100, Chemicon) were performed.

Both D-4F and L-4F have robust anti-inflammatory properties (56–58), improve HDL function (56, 59–63), and increase cholesterol efflux (37, 38). In this study, to identify whether D-4F/L-4F can pass the BBB and enter the brain, two ABCA1$^{fl/fl}$-T2DM-stroke mice were subcutaneously administered saline or commercially available FITC-D-4F (Cat#SP160428, Lot#P160412-LR051957, BioMatik, Cambridge, ON, Canada) at 24 and 48 h after dMCAo. Mice were sacrificed 4 h after last treatment and vibratome coronal sections (100 μm) were prepared for immunostaining with vWF, APC, and neuronal nuclei (NeuN, for neurons, 1:300, MAB 377, Chemicon). Images were analyzed using laser scanning confocal microscopy.

For immunostaining measurement, each section containing 8 fields of view within the cortex and corpus callosum (CC) from the ischemic boundary zone (IBZ) were digitized using a 40× objective (Olympus BX40) using a 3-CCD color video camera (Sony DXC-970MD) interfaced with MCID. The percentage of positively stained area for albumin, Occludin, AQP-4, BS, LFB, and SMI-31 was measured using a built-in densitometry function (MCID) with a uniform threshold set above unstained for all the groups and the number of vWF$^+$-vessels, αSMA$^+$-arterioles, APC$^+$-OLs, PDGFR$^+$-OPCs and the perimeter of vessels or diameter of arterioles as well as the number of αSMA$^+$-SMCs was measured in both the contralateral and the ipsilateral brain.

Quantification of Myelination on Electronic Microscope Images

To evaluate the ultrastructure of axonal myelination, brain tissues were isolated from the IBZ of CC and processed to ultrathin sections for EM analysis (n = 6 mice/group). Axonal structural changes were identified at a magnification of 14,000× in a total of 6 fields of view per animal. The analysis included measurement of the percentage of myelinated axons, thickness of myelin sheath, and G ratio (axon diameter/axon wrapped with myelin diameter × 100%) in 10 ultrathin sections, as described previously (36).

Western Blot and Real-Time Quantitative PCR (RT-PCR) Assay

Tissue from the ischemic area of the ipsilateral hemisphere from both vehicle-control and L-4F-treated T2DM stroke mice were isolated at 21 days after dMCAo. Brain-tissue lysate was subjected

to WB analysis, as described previously (46, 64). The following primary antibodies were used: AQP4 (1:5,000, Milipore, cat# ab3594), myelin basic protein (MBP, 1:500, Millipore, cat# MAB386), CD68 (ED-1, a marker of M1-macrophages, 1:1,000, Serotec, cat# MCA341R), monocyte chemoattractant protein-1 (MCP-1, 1:1,000, Abcam, cat# ab7202), toll-like receptor 4 (TLR4, 1:500, Santa Cruz, cat# sc-10741), Insulin-like growth factor 1 (IGF-1, 1:500, Santa Cruz, cat# sc-9013), IGF-1 receptor β (TGF-1Rβ,1:500, Santa Cruz, cat# sc-713), and β-actin (1:10,000, Abcam, cat# ab6276).

Total RNA was isolated using a standard protocol and quantitative RT-PCR was performed on an ABI Prism 7,000 Sequence Detection System using the Power SYBR Green PCR Master Mix (Applied Biosystems, Foster City, CA). For each sample, the cDNA was generated and used to amplify GAPDH, AQP4, MBP, ED1, MCP-1, TLR4, IGF1, and IGF-1R as described previously (46). All the primers for the RT-PCR assay were designed using Primer Express software (ABI). Each sample was detected in triplicates.

Statistical Analysis

A total of two-way ANOVA followed by Tukey *post hoc* Test were used for analysis involving four groups, i.e., ABCA1$^{fl/fl}$-T2DM and ABCA1$^{-B/-B}$-T2DM stroke with or without L-4F treatment for analysis blood biochemistry, hemorrhage, mortality, lesion volume, functional outcome, immunostaining, EM measurement, WB and RT-PCR measurement. $p < 0.05$ was set as a significant difference, and all data are presented as mean ± standard error (SE).

In this study, 9 survival animals in each group were employed for the measurement of hemorrhage and lesion volume, and histochemical and immunohisto-staining measurements. The number of animals employed was determined using a priori power calculation; 9 survival stroke animals per group provided 80% power at a significance level of <0.05, assuming a 20% difference in both mean and SD at the 95% CI and a two-sided test. For WB, RT-PCR, and EM analysis, 6 stroke mice per group were needed. Plus, two additional ABCA1$^{fl/fl}$-T2DM-stroke mice, in this study, a total of 86 T2DM-stroke mice were used.

RESULTS

L-4F-Treatment Decreases Blood Glucose, Cerebral Hemorrhage, and Mortality, Increases HDL and Improves Functional Outcome After Stroke in T2DM Mice

Figure 1 shows that there were no significant differences in the blood levels of glucose before treatment and triglyceride and T-CH at 21 days after treatment among the 4 groups of animals treated with or without L-4F for 21 days after dMCAo. However, L-4F treatment significantly increased blood HDL level and decreased glucose ($p < 0.05$, $n = 21$/group). ABCA1$^{-B/-B}$-T2DM mice exhibit increased hemorrhage, lesion volume, and mortality compared to ABCA1$^{fl/fl}$-T2DM-stroke mice ($p < 0.05$, $n = 9$/group). There were no changes in lesion

volume at 21 days after L-4F treatment in both the ABCA1$^{-B/-B}$-T2DM and the ABCA1$^{fl/fl}$-T2DM-stroke mice. However, the hemorrhage volume and mortality rate was dramatically reduced in L-4F treatment groups in both ABCA1$^{fl/fl}$ and ABCA1$^{-B/-B}$ T2DM-stroke mice when compared to the vehicle control group, respectively ($p < 0.05$).

ABCA1$^{-B/-B}$-T2DM stroke mice exhibited significant functional deficits as indicated by increased adhesive-removal time on 3, 7, 14, and 21 days after dMCAo compared with ABCA1$^{fl/fl}$-T2DM mice ($p < 0.05$, $n = 21$/group). L-4F treatment significantly reduced adhesive-removal time at 14 and 21 days after stroke indicating improved sensorimotor function and decreased the left foot-fault rate at 7, 14, and 21 days after treatment indicating an improved motor function in both ABCA1$^{fl/fl}$ and ABCA1$^{-B/-B}$ T2DM-stroke mice ($p < 0.05$, $n = 21$/group). These data indicate that L-4F treatment increases blood HDL and reduces glucose levels, decreases cerebral hemorrhagic transformation and mortality as well as improves neurological functional outcomes in T2DM-stroke mice.
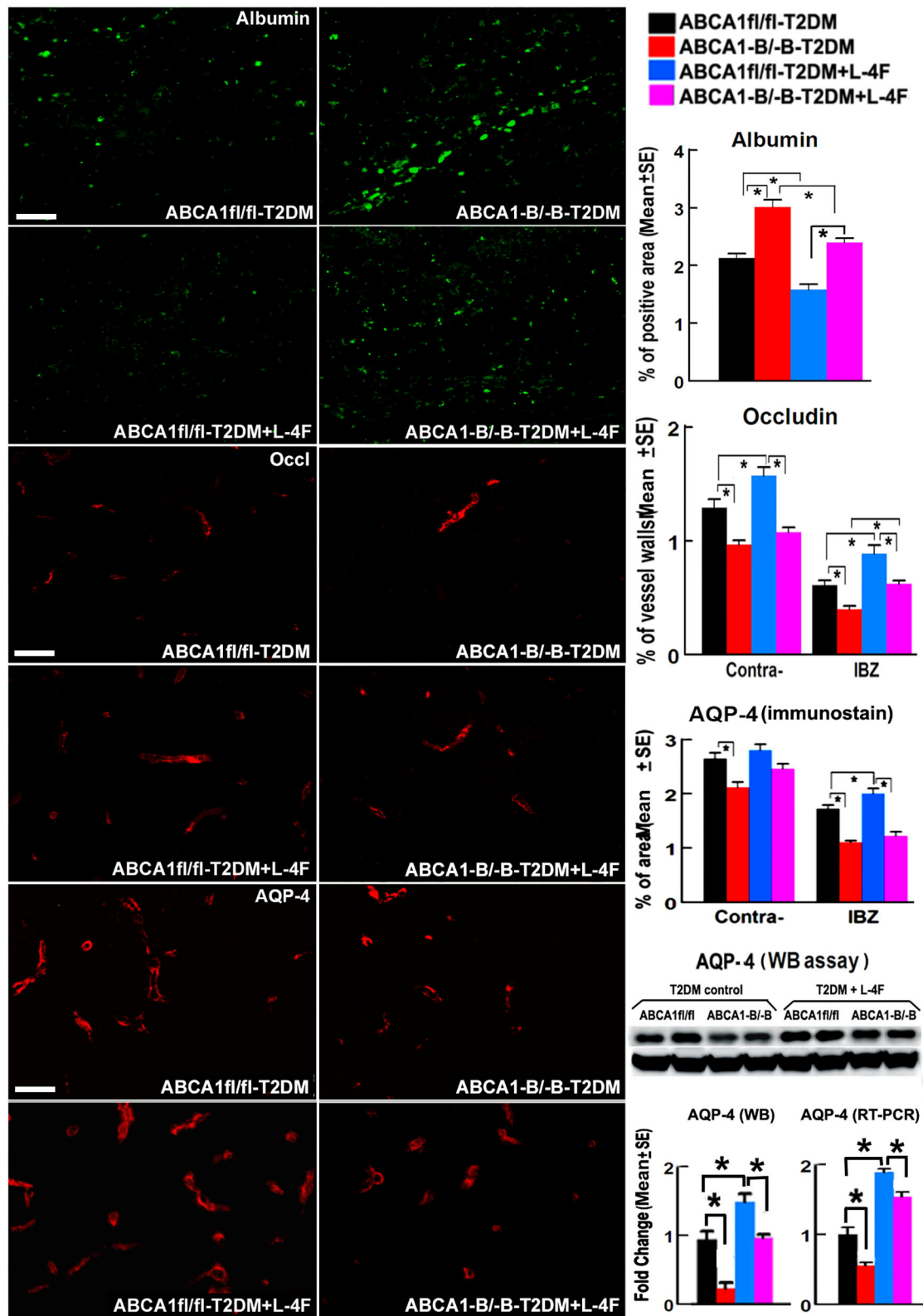
L-4F Treatment Decreases BBB Leakage and Cerebral Vascular Damage in the Ischemic Brain of T2DM-Stroke Mice

Figure 2 shows that the density of albumin in the ischemic core area increased in ABCA1$^{-B/-B}$-T2DM stroke mice, while the expression of Occludin and AQP-4 within or around blood vessels in both the contralateral and the IBZ area in the ABCA1$^{-B/-B}$-T2DM stroke mice significantly decreased compared with the ABCA1$^{fl/fl}$-T2DM stroke mice ($p < 0.05$, $n = 9$/group). In addition, WB and RT-PCR assay indicate that the level of AQP-4 in the ischemic brain is decreased in the ABCA1$^{-B/-B}$-T2DM stroke mice ($p < 0.05$, $n = 6$/group). L-4F treatment significantly decreased albumin density indicating improved BBB integrity and increased tight junction protein in the ischemic brain in both ABCA1$^{-B/-B}$ and ABCA1$^{fl/fl}$ T2DM-stroke mice measured by immunostaining ($p < 0.05$, $n = 9$/group). Moreover, L-4F treatment also elevated AQP4 expression in the ischemic brain tissues measured by WB and RT-PCR ($p < 0.05$, $n = 6$/group) even though there is no significant difference by immunostaining analysis.
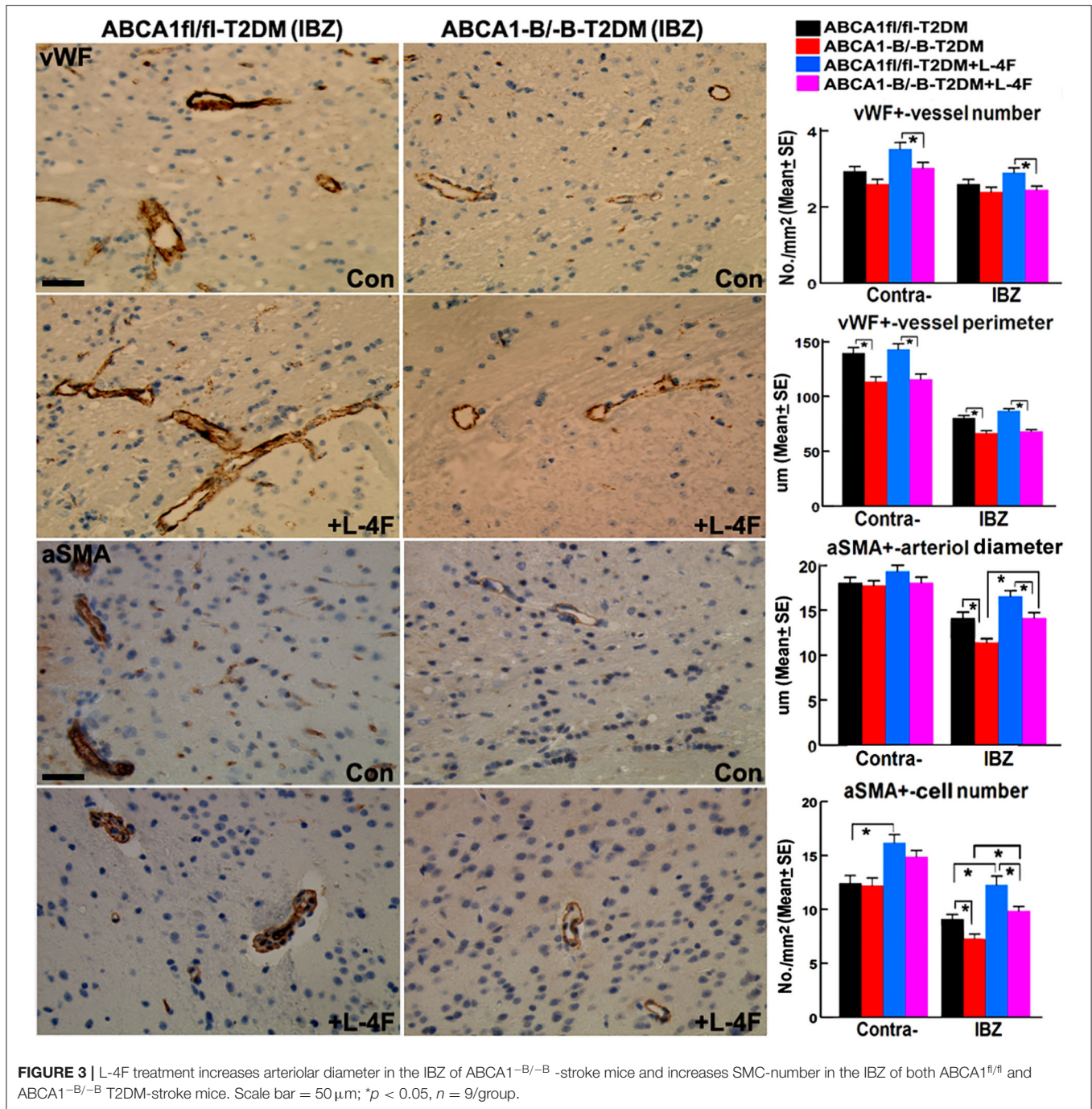
Figure 3 shows that even though there were no significant differences in the densities of vWF$^+$-vessels and αSMA$^+$-arterioles in both the contralateral hemisphere and the IBZ, and the diameter of arterioles and the number of αSMA$^+$-SMCs in the contralateral hemispheres between the ABCA1$^{-B/-B}$ and ABCA1$^{fl/fl}$ T2DM-stroke mice, ABCA1$^{-B/-B}$-T2DM stroke mice exhibit decreased vessel perimeter in both the contralateral hemisphere and the IBZ, and decreased arteriole diameter and SMC number in the IBZ compared with ABCA1$^{fl/fl}$-T2DM stroke mice ($p < 0.05$, $n = 9$/group). L-4F treatment increased the number of SMCs in both the contralateral hemisphere and IBZ of ABCA1$^{fl/fl}$-T2DM mice and increased SMC number and arteriole diameter in the IBZ of ABCA1$^{-B/-B}$-T2DM stroke mice 21 days after stroke ($p < 0.05$, $n = 9$/groups). These data indicate that T2DM-stroke induces BBB leakage and vascular injury in the ischemic brain, while brain-ABCA1 deficit exacerbates
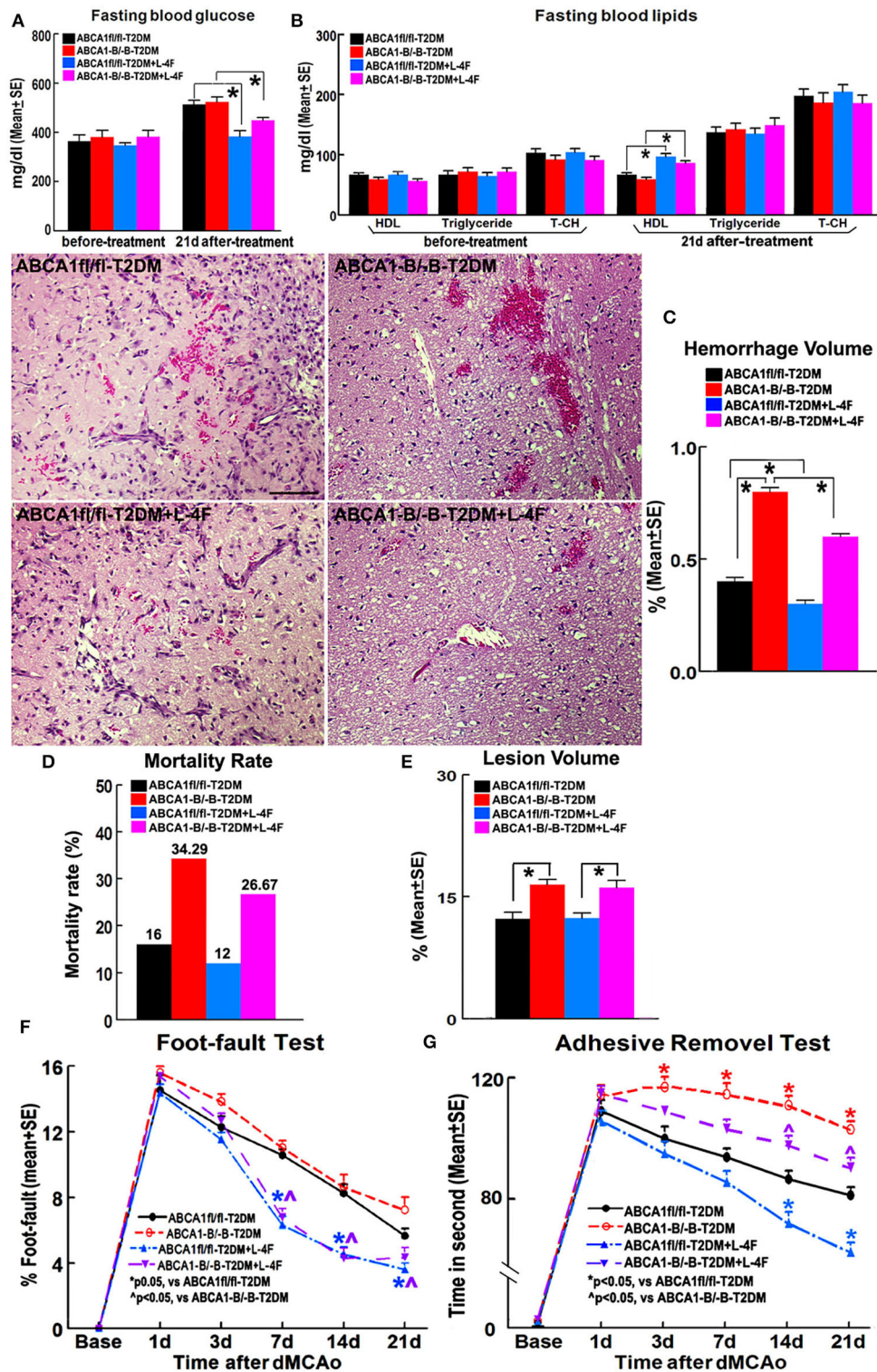
FIGURE 1 | L-4F treatment does not change blood glucose levels before treatment and T-CH and triglyceride after treatment. However, L-4F treatment significantly reduces glucose and increases HDL in the blood 21 days after treatment. L-4F treatment does not alter lesion volume but reduces cerebral hemorrhage and mortality rate as well as improves functional outcome compared with vehicle-control groups in both ABCA1$^{-B/-B}$ and ABCA1$^{fl/fl}$ T2DM-stroke mice, respectively. **A,B** Fasting blood levels of glucose **(A)** and lipids **(B)** measured before L-4F treatment at 1 day after dMCAo and 21 days after treatment. $p < 0.05$, $n = 21$/group; **C–E** Cerebral hemorrhage volume **(C)**, mortality **(D)**, and lesion volume **(E)** at 21 days after L-4F treatment. Scale bar = 100 μm; $p < 0.05$, $n = 9$/group; **F,G.** Foot-fault **(F)** and adhesive removal **(G)** tests before dMCAo and 1, 3, 7, 14, and 21 days after dMCAo. *$p < 0.05$, $n = 21$/group.

FIGURE 2 | L-4F treatment decreases BBB-leakage (albumin density) but increases tight-junction protein (Occludin) in the ischemic brain of T2DM mice at 21 days after stroke. L-4F treatment did not show an increases AQP-4 expression in astrocyte end-feet measured by immunostaining. However, the WB and RT-PCR data demonstrate that both the protein and mRNA level of AQP-4 in the ischemic brain was increased after 21 days of L-4F treatment. Scale bar = 50 μm; *$p < 0.05$, $n = 9$/group in immunostaining measurement of Albumin, Occludin and AQP-4, $n = 6$/group in WB and RT-PCR assay.

FIGURE 3 | L-4F treatment increases arteriolar diameter in the IBZ of ABCA1$^{-B/-B}$ -stroke mice and increases SMC-number in the IBZ of both ABCA1$^{fl/fl}$ and ABCA1$^{-B/-B}$ T2DM-stroke mice. Scale bar = 50 μm; *$p < 0.05$, $n = 9$/group.

T2DM-stroke induced vascular damage. Administration of L-4F decreased T2DM-stroke induced vascular damage and BBB permeability even in brain-ABCA1-deficient mice.

## L-4F Treatment Increases WM Density and Oligodendrogenesis in the Ischemic Brain of T2DM-Stroke Mice

The immunohisto-chemical-staining and quantification data show that the ABCA$^{-B/-B}$-T2DM stroke mice exhibit a significant decrease in the densities of axons, phosphorylated-neurofilament, and myelin in the WM-bundles of CC (**Figure 4**, $p < 0.05$, $n = 9$/group), and WB/RT-PCR assay show that the protein and mRNA level of MBP was decreased in the ischemic brain tissues (**Figure 4**, $p < 0.05$, $n = 6$/group) at 21 days after dMCAo compared with the ABCA1$^{fl/fl}$-T2DM stroke mice. The analysis from EM images indicates that both the number of myelinated-axons and the thickness of myelin-sheath decreased but G-ratio increased in the WM-bundles of CC in both the contralateral brain and the IBZ of the ischemic brain
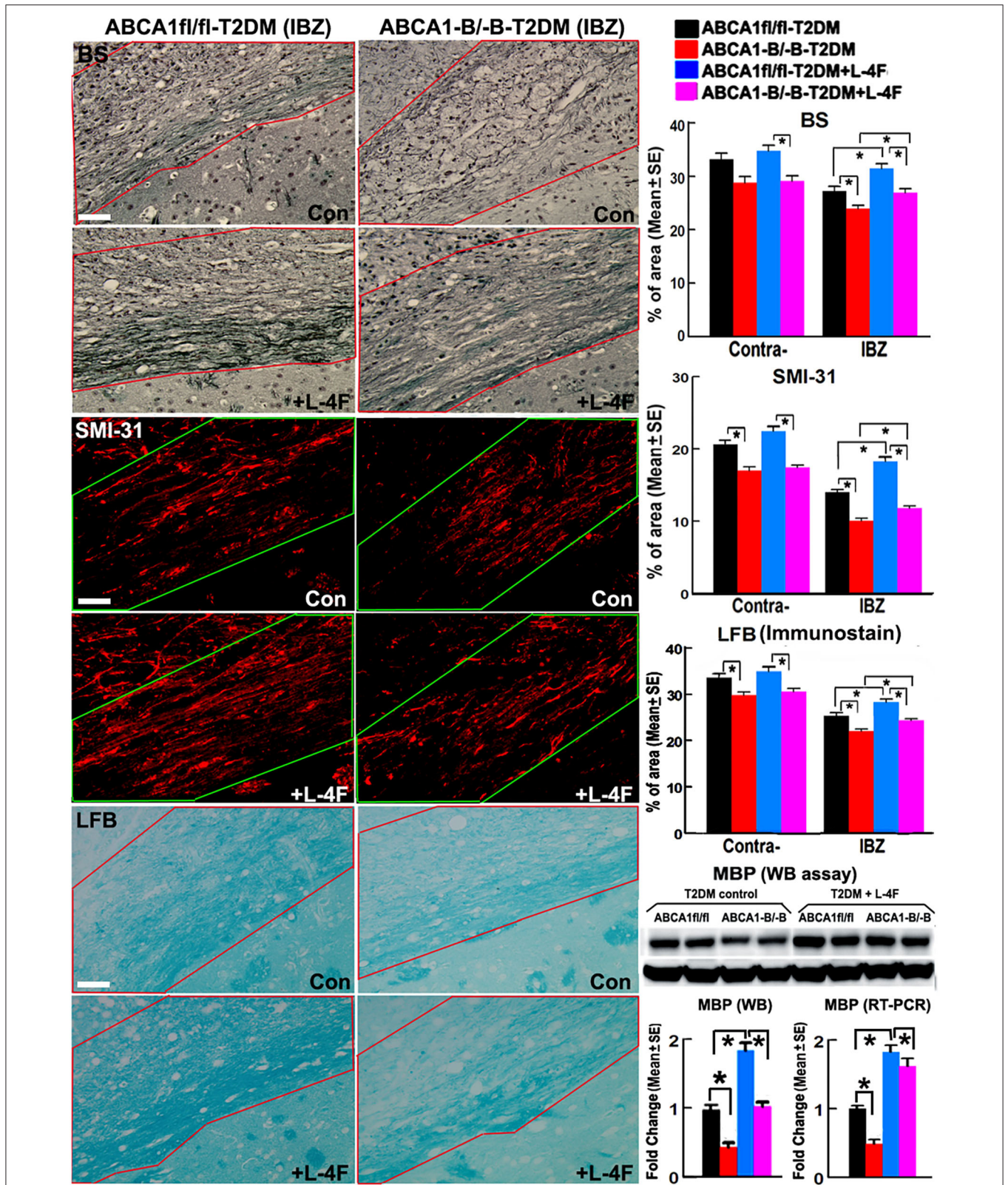
FIGURE 4 | L-4F treatment increases the densities of axon, phospho-neurofilament, and myelin in the WM-bundles in the IBZ, and MBP protein level in the ischemic brain of ABCA1^{fl/fl} and ABCA1[−B/−B] T2DM mice at 21 days after stroke. Scale bar = 50 μm. *$p < 0.05$, $n = 9$/group in immunostaining measurement; $n = 6$/group in WB and RT-PCR assay.
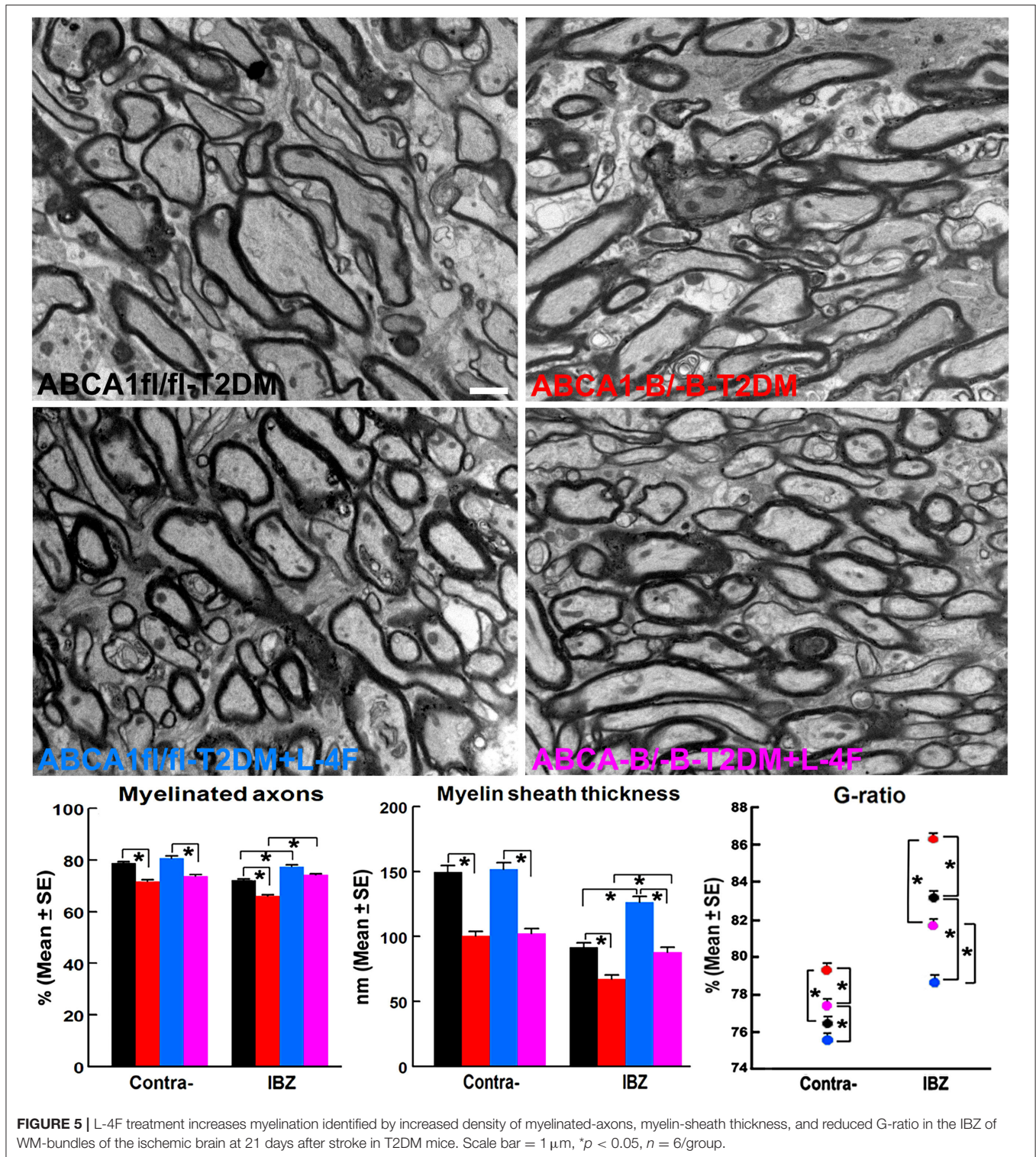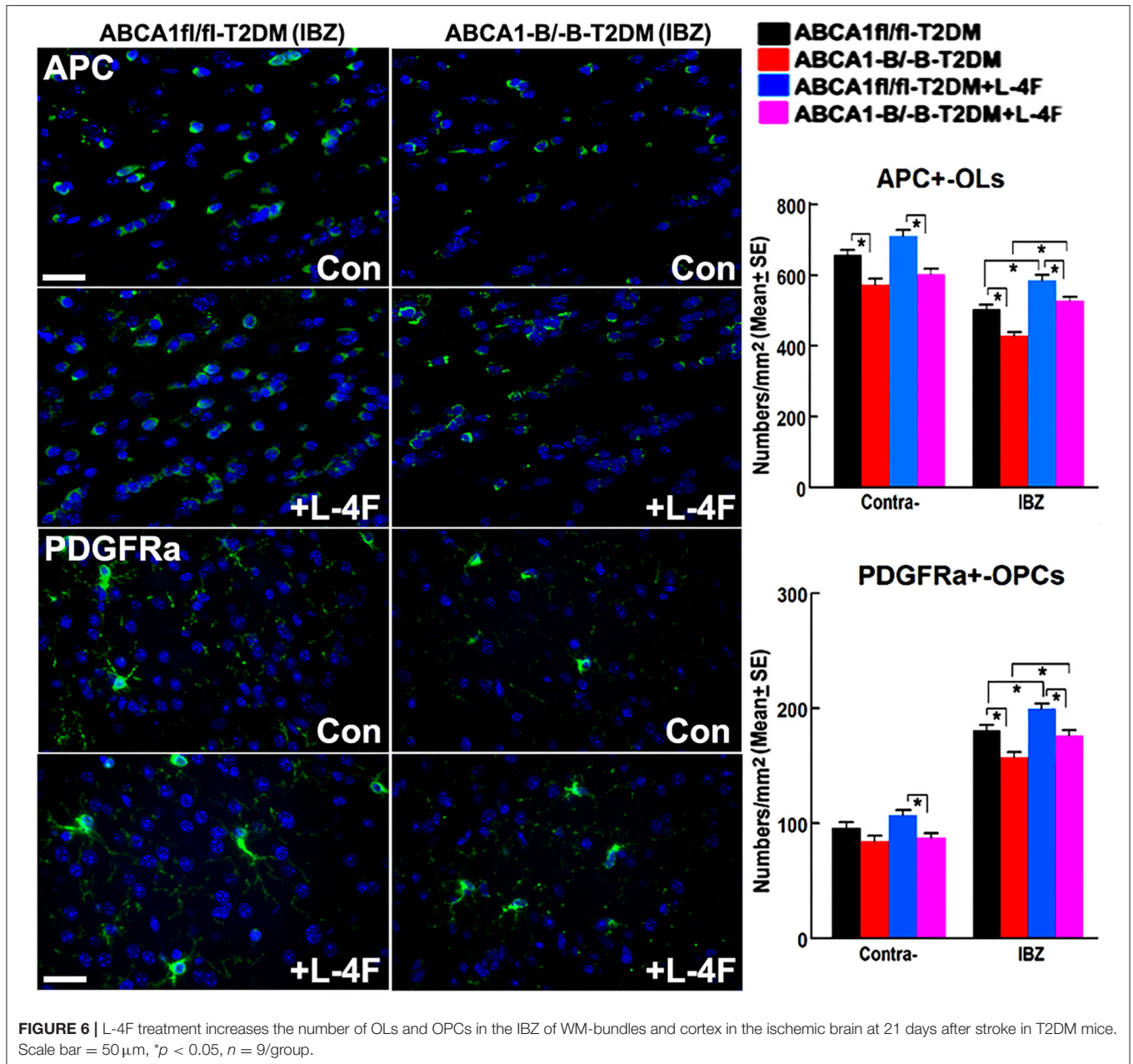
FIGURE 5 | L-4F treatment increases myelination identified by increased density of myelinated-axons, myelin-sheath thickness, and reduced G-ratio in the IBZ of WM-bundles of the ischemic brain at 21 days after stroke in T2DM mice. Scale bar = 1 μm, *$p < 0.05$, n = 6/group.

in the ABCA$^{-B/-B}$-T2DM stroke mice (**Figure 5**, $p < 0.05$, n = 6/group). Moreover, the number of APC$^+$-OLs in the CC of the IBZ and the number of PDGFRα$^+$-OPCs in the cortex of the IBZ of ABCA$^{-B/-B}$-T2DM stroke mice were also reduced (**Figure 6**, $p < 0.05$, n = 9/group). L-4F treatment significantly

decreased G-ratio, increased the axon density, phosphorylated-neurofilaments, myelin density, number of myelinated-axons, myelin-sheath thickness, and the number of OLs and OPCs in the IBZ ($p < 0.05$, n = 9/group) and also the protein/mRNA levels of MBP in the ischemic brain tissues ($p < 0.05$, n = 6/group) in both

FIGURE 6 | L-4F treatment increases the number of OLs and OPCs in the IBZ of WM-bundles and cortex in the ischemic brain at 21 days after stroke in T2DM mice. Scale bar = 50 μm, *$p < 0.05$, n = 9/group.

ABCA1$^{fl/fl}$-T2DM and ABCA$^{-B/-B}$-T2DM stroke mice when compared with the vehicle-control group, respectively. These data indicate that L-4F treatment promotes WM remodeling and oligodendrogenesis in the ischemic brain after stroke in T2DM mice.

Identification of Localization of FITC-Labeled D-4F After Treatment

Figure 7 shows that the FITC-labeled D-4F can pass through the BBB to enter the ischemic lesion area and was primarily present in vWF$^+$-vessels and APC$^+$-OLs and NeuN$^+$-neurons in the ischemic brain.

L-4F Treatment Reduces Macrophage Infiltration and Decreases Inflammation in the Ischemic Brain in T2DM-Stroke Mice

To investigate the mechanism underlying L-4F treatment-induced neurorestoration in T2DM-stroke, the macrophage/microglial and monocyte infiltration was measured using the levels of ED-1 and MCP-1, and the inflammatory factor TLR-4 and anti-inflammatory factors IGF-1 and IGF-1Rβ were measured using WB and RT-PCR assay. **Figure 8** shows that the ABCA$^{-B/-B}$-T2DM stroke mice exhibit an increased level of protein and mRNA of ED-1, MCP-1, and TLR-4, whereas a lower level of IGF-1/IGF-1Rβ in
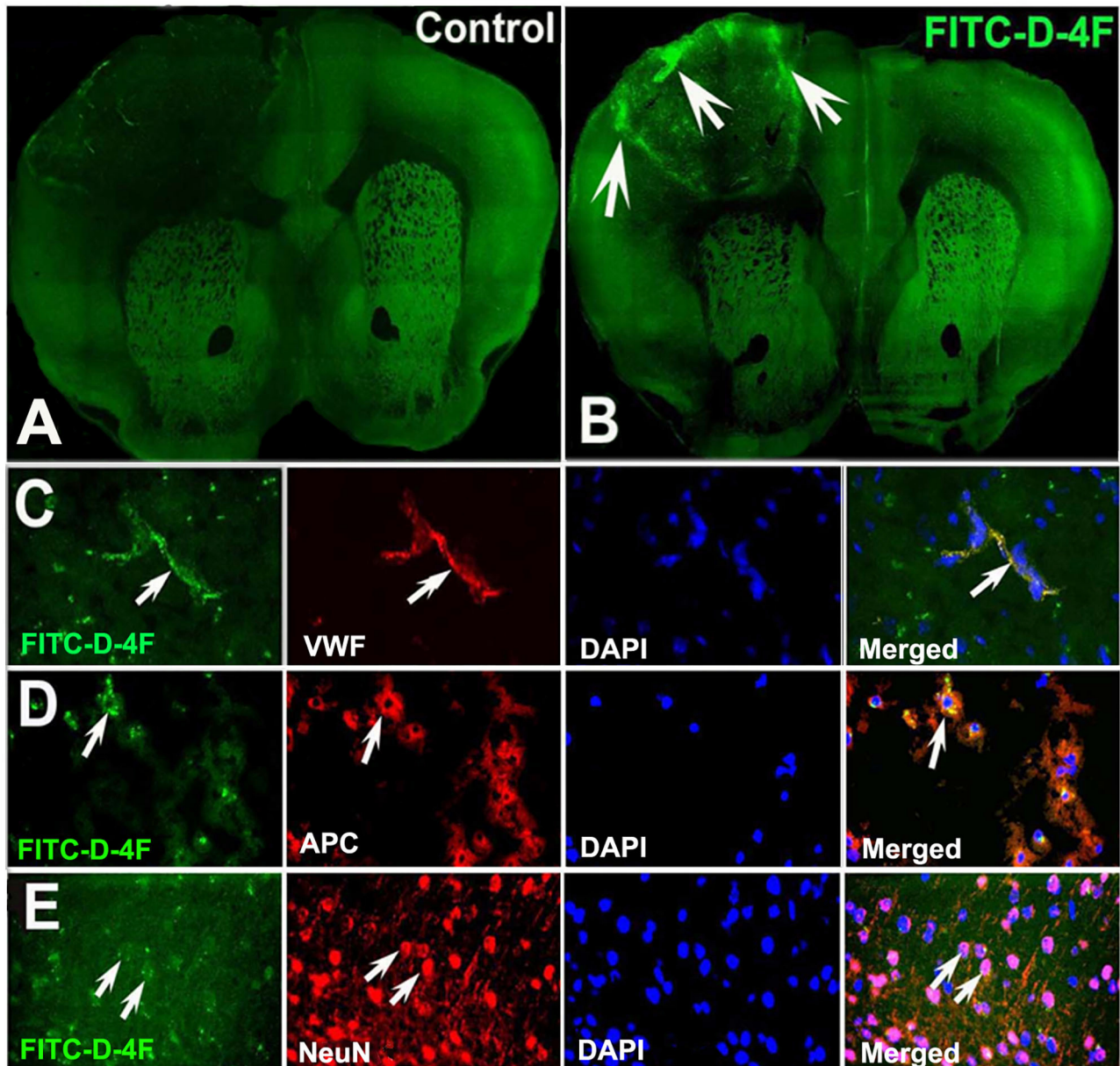
FIGURE 7 | D-4F can pass through the BBB and enter into the ischemic brain, and was co-localized with vWF+-vessels, APC+-OLs, and NeuN+-neurons in the IBZ of the ischemic brain of T2DM-stroke mice. The confocal image of mouse brain in control **(A)** and FITC-D-4F **(B)**. D-4F was co-localized with vascular vessels **(C)**, OLs **(D)** and neurons **(E)**, respectively.

the ischemic brain tissues when compared that with the ABCA1$^{fl/fl}$-T2DM stroke mice at 21 days after dMCAo ($p < 0.05$, $n = 6$/group). L-4F treatment significantly decreases ED-1, MCP-1, and TLR-4 expression and increases IGF-1 and IGF-1Rβ levels in the ischemic brain compared with the vehicle-control group, respectively ($p < 0.05$, $n = 6$/group). These data indicate that post-stroke administration of L-4F in T2DM-stroke mice inhibits neuroinflammation which may contribute to the L-4F treatment-induced neurorestoration after brain injury.

DISCUSSION

The BBB contains vascular endothelial cells (ECs), pericytes, tight junction, and astrocyte end-feet and interacts directly with astrocytes and neurons in the neurovascular niche (65–67). The BBB acts selectively as a transport interface and therapeutic agents must pass the BBB to provide successful treatment of brain injury or disease (67). Using commercially available FITC-labeled D-4F, we demonstrated that D-4F/L-4F can pass through the BBB to enter brain tissue and cells including ECs, OLs, and neurons.
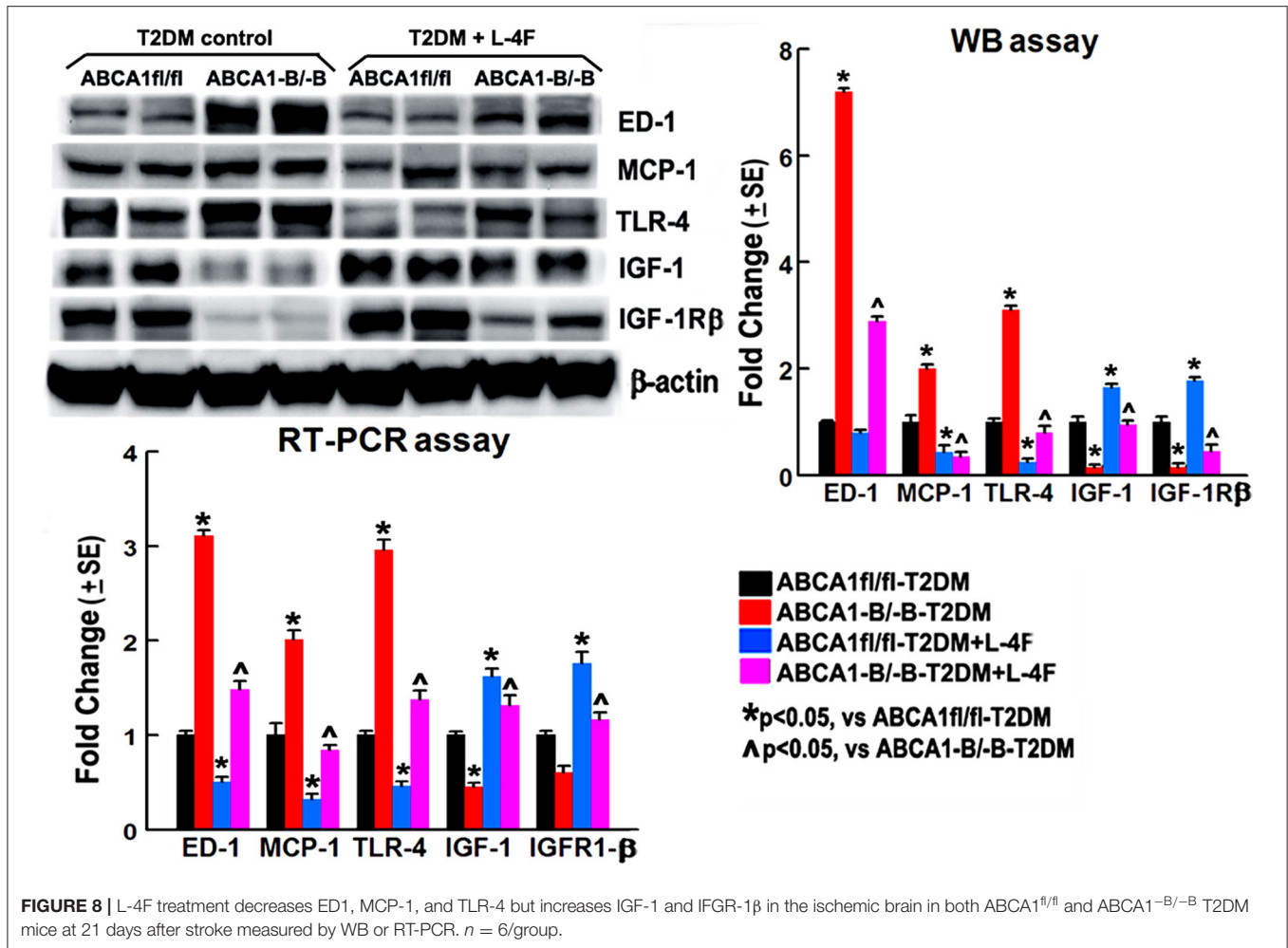
FIGURE 8 | L-4F treatment decreases ED1, MCP-1, and TLR-4 but increases IGF-1 and IFGR-1β in the ischemic brain in both ABCA1^{fl/fl} and ABCA1[−B/−B] T2DM mice at 21 days after stroke measured by WB or RT-PCR. $n = 6$/group.

Long-term endothelial dysfunction and impaired vasodilation, as well as increased vasogenic edema and BBB leakage in the ischemic brain, are highly associated with T2DM as a predictor for secondary cerebrovascular events such as hemorrhage (68). Neurovascular dysfunction triggers and exacerbates WM damage which in turn hinders neurological functional recovery, and leads to an enlarged infarct volume after stroke in both the experimental T2DM-stroke model and T2DM-stroke patients (51, 64, 69–73). In this study, we demonstrate that L-4F treatment not only has beneficial effects on BBB integrity (identified by decreased albumin infiltration, increased tight junction protein expression, and AQP-4 expression in astrocyte end-feet), but also on neurovascular remodeling (identified by increased SMC number and enhanced vasodilation), WM remodeling (identified by increased WM density and myelination), and oligodendrogenesis (identified by the increased number of OLs and OPCs) in the ischemic brains in the middle-aged wild-type (ABCA^{fl/fl}) T2DM-stroke mice. These results are consistent with our previous findings that treatment of db/db-T2DM stroke mice with L-4F reduced hemorrhage, infarct volume, mortality, BBB leakage and WM damage, and increased cerebral arteriole diameter and SMC number in the ischemic brain 4

days after stroke (46). We also found previously that *in vitro*, L-4F treatment does not increase angiogenesis in mouse-brain ECs cultured in high-glucose media, but increases primary artery explant cell migration after stroke-induced injury and enhances neurite and axonal outgrowth in primary cortical neurons subjected to oxygen-glucose deprivation or high glucose (46). D-4F treatment of T1DM-stroke rats also increases tight junction protein expression and decreases BBB leakage, WM damage, and pro-inflammatory factors, while increasing anti-inflammatory M2 macrophage polarization in the ischemic brain 7 days after stroke (45). L-4F decreases markers of plasma oxidation and promotes EC migration and EC-healing of carotid arterial injuries in HFD-fed mice (74). L-4F-treated mice exhibit reduced serum levels of oxidized phospholipids and increased mean αSMA[+]-area in the aortic lesion in a murine lupus model of accelerated atherosclerosis (75).

In the peripheral blood system, ApoA-I is a major apolipoprotein involved in HDL formation and is highly influenced by ABCA1, and ABCA1 is usually found in tissue macrophages and activated monocytes (39, 76–80). In the CNS, HDL synthesis uses ApoE as the predominant apolipoprotein regulated by ABCA1 *via* facilitating cholesterol and phospholipid

efflux to exogenous ApoE (81–83), and ABCA1 is also highly expressed in neurons, astrocytes, OLs, and microglia (26, 29, 84–87). D-4F promotes cholesterol efflux from macrophages *via* ABCA1 (42). In this study, L-4F treatment increases blood HDL in ABCA$^{fl/fl}$-T2DM stroke mice. Since L-4F can cross the BBB and reach the CNS, to further elucidate whether L-4F treatment-induced neurorestorative effect on T2DM-stroke is mediated by ABCA1 and ApoE signaling pathway, ABCA$^{-B/-B}$ mice were employed. These mice were generated by crossing loxP-flanked (floxed) ABCA1 mice with nestin-cre mice, by which the ABCA1 gene is knocked out from all nestin-linage cells (neural stem cells) in the brain including neurons, OLs, and astrocytes, and these mice exhibit reduced brain ABCA1 and ApoE and HDL content, and reduced level of ABCA1, ApoE and HDL was also found in a primary cortical neuron or OPC cultures (17, 29, 34–36, 47). Our results indicate that inhibition of brain ABCA1 does not attenuate the neurorestorative benefits induced by L-4F treatment in ABCA$^{-B/-B}$-T2DM stroke mice. D-4F is capable of forming HDL-like particles and delivering cholesterol to the liver cells selectively through the scavenger receptor class B type I (SR-BI) and enhances the cholesterol delivery by native HDL (40). D-4F treatment increases Lecithin cholesterol acyltransferase activity, increases HDL levels and cholesterol efflux from macrophages, decreases inflammation and oxidative stress, improves renal histological pathogenesis, and causes lesion regression in ApoE(-/-) mice (38, 88–90). D-4F also improves arterial vasoreactivity and arterial wall thickness in hypercholesterolemic LDLR(-/-) mice and LDLR(-/-) and ApoA-I(-/-) double-knockout mice which independent of ApoA-I (59, 91). Administration of L-4F increases HDL and ApoA-I concentration in the plasma, decreases albuminuria and stimulates cholesterol efflux and related proteins expressions, and reduces atherosclerotic lesions in ApoE (-/-) mice (39, 43, 92). GW3965, an LXR agonist increases ApoA-I protein levels in the CNS independent of ABCA1, which suggests that ApoA-I may be regulated by distinct mechanisms on either side of the BBB and that ApoA-I may serve to integrate peripheral and CNS lipid metabolism (27). This study along with previous studies suggests that L-4F derived therapeutic effects in brain rewiring after stroke injury may, at least partially, be independent of the ABCA1, ApoE, or ApoA-I.

Compared with non-DM stroke, T2DM stroke have chronic states of oxidative stress and inflammation, which is highly associated with extensive microvascular and WM damage (14, 50, 64, 93–97). Some studies report that D-4F and L-4F have no effect on blood lipid, T-CH, or HDL levels but improve HDL function in anti-oxidation and anti-inflammation in both the peripheral and cerebral vascular systems (37, 38, 56, 59–63, 74, 93, 98–102), which implies that D-4F and L-4F, similar to HDL, have neuroprotective and neurorestorative potential in atherosclerosis (37, 92, 101, 103–105), diabetes (101, 106, 107), and ischemic stroke (45, 46). L-4F has the ability to preferentially bind to proinflammatory oxidized lipids and decrease serum and endothelium oxidized-LDL levels and improve vasodilation by stimulation of the arterial wall cells including ECs and SMCs in both wild-type and LDLR(-/-) mice fed with or without HFD food (56–58, 108–111). Administration of D-4F improved the

migration of ECs and angiogenesis, alleviated oxidative stress (107), and decreased circulating EC sloughing, superoxide anion levels, and vasoconstriction in diabetic rats, which are associated with an increase in antioxidant proteins, HO-1 and EC-SOD (93). D-4F and L-4F have the ability to inhibit LDL-induced monocyte chemotactic activity *via* inhibiting MCP-1, a key chemokine that regulates migration and infiltration of monocytes and macrophages, production in cultures of human aortic ECs (100, 112). D-4F suppressed IL-4-induced macrophage alternative activation and pro-fibrotic TGF-β1 expression (113) and L-4F-reduced vascular cell adhesion molecule-1 expression in lipopolysaccharide (LPS)-induced inflammatory responses (114). D-4F treatment evokes a vascular protective role in LPS-induced acute lung injury by improving the endothelial progenitor cell (EPC) numbers, differentiation, and function, and decreasing plasma levels of the pro-inflammatory mediators such as TNF-α and ET-1 partially *via* the PI3K/AKT/eNOS signaling pathway (115). D-4F treatment also reduces infiltration of macrophages in diabetic ApoE-/- mice (101), and also decreases arterial macrophage traffic and inflammatory factors such as IL-1β, IFN-Υ, and TNFα on HFD-fed mice or rabbits (106, 116, 117), In thisstudy, L-4F treatment decreased the infiltration of M1-macrophages, MCP-1, and TLR-4 (a key inflammatory factor expressed in M1-macrophages whose activation leads to activation of the intracellular signaling pathway NFκB and inflammatory cytokine production), while increasing IGF-1 and IGF-1Rβ in the ischemic brain in both ABCA$^{fl/fl}$ and ABCA$^{-B/-B}$ mice. These results are consistent with our previous findings that D-4F treatment of T1DM rats decreases MMP9 and proinflammatory mediators TNFα, TLR-4 and increases anti-inflammatory M2-macrophage polarization (45). Administration of L-4F to db/db T2DM stroke mice mitigated macrophage infiltration and reduced TNFα (46) in the ischemic brain. IGF1 is involved in neurogenesis, oligodendrogenesis, and myelination (118), and reduces stroke-induced BBB damage and sustained antiinflammation in the brain (119). IGF1 also decreases cholesterol efflux *via* ABCA1 and SR-BI expression (120). Similarly, in T2DM patients L-4F treatment restored the HDL anti-inflammatory index in diabetic plasma samples (121).

In this study, L-4F-treated T2DM-stroke animals also exhibit decreased blood glucose level, which is consistent with our previous results that L-4F decreased high-mobility group box-1 (HMGB-1), advanced glycation end-product receptor (RAGE), and plasminogen activator inhibitor-1 (PAI-1) in the ischemic brain in T2DM-stroke mice (46). D-4F treatment also increased blood glucose clearance and improve insulin tolerance in HFD-fed mice (106) and D-4F treatment ameliorated disordered glycolysis impaired by ox-LDL (107). Whether L-4F treatment-induced neurorestorative benefits are due to blood glucose regulation warrants future investigation.

Summary

In this study, we demonstrate that L-4F can pass through the BBB and has neurorestorative benefits such as promoting neurovascular and WM remodeling and oligodendrogenesis in the ischemic brain as well as improvement of neurological

functional recovery in T2DM-stroke mice. L-4F-treated T2DM-stroke mice exhibit suppressed neuroinflammation in the ischemic brain of both ABCA1$^{-B/-B}$ and ABCA1$^{fl/fl}$ T2DM stroke mice. These findings indicate that post-stroke administration of L-4F may provide a potential strategy for neurorestoration following stroke injury in the T2DM population, and reducing neuroinflammation in the injured brain may contribute to the neurorestorative effects of L-4F at least partially independent of the ABCA1 signaling pathway.

Limitation

In this study, all brain tissue samples were collected 21 days after stroke. Tissue sampling at this late time point enables the study of long-term vascular and WM remodeling effects in the brain, however, from this delayed sampling we are unable to glean information of BBB leakage and inflammatory responses at the acute phase of stroke recovery, which warrants future investigation.

DATA AVAILABILITY STATEMENT

The raw data supporting the conclusions of this article will be made available by the authors, without undue reservation.

ETHICS STATEMENT

The animal study was reviewed and approved by Institute of Animal Care and Use Committee of the Henry Ford Health System.

AUTHOR CONTRIBUTIONS

XC and QJ conceived and designed this study. MZ, RL, AZ, YQ, JL-W, PV, and XC performed mouse experiments, acquisition of data, and statistical analysis. XC wrote and prepared this manuscript. PV and MC made critical revisions of the manuscript for intellectual content. All authors read and approved the final manuscript.

REFERENCES

1. Putaala J, Liebkind R, Gordin D, Thorn LM, Haapaniemi E, Forsblom C, et al. Diabetes mellitus and ischemic stroke in the young: clinical features and long-term prognosis. *Neurology.* (2011) 76:1831–7. doi: 10.1212/WNL.0b013e31821cccc2

2. Araki A, Iimuro S, Sakurai T, Umegaki H, Iijima K, Nakano H, et al. Non-high-density lipoprotein cholesterol: an important predictor of stroke and diabetes-related mortality in Japanese elderly diabetic patients. *Geriatr Gerontol Int.* (2012) 12 (Suppl. 1):18–28. doi: 10.1111/j.1447-0594.2011.00809.x

3. Megherbi SE, Milan C, Minier D, Couvreur G, Osseby GV, Tilling K, et al. Association between diabetes and stroke subtype on survival and functional outcome 3 months after stroke: data from the European biomed stroke project. *Stroke.* (2003) 34:688–94. doi: 10.1161/01.STR.0000057975.15221.40

4. Singh P, Aronow WS, Mellana WM, Gutwein AH. Prevalence of appropriate management of diabetes mellitus in an academic general medicine clinic. *Am J Ther.* (2010) 17:42–5. doi: 10.1097/MJT.0b013e3181822e78

5. Hong P, Gu RN, Li FX, Xiong XX, Liang WB, You ZJ, et al. NLRP3 inflammasome as a potential treatment in ischemic stroke concomitant with diabetes. *J Neuroinflam.* (2019) 16:121. doi: 10.1186/s12974-019-1498-0

6. Tuttolomondo A, Puleo MG, Velardo MC, Corpora F, Daidone M, Pinto A. Molecular biology of atherosclerotic ischemic strokes. *Int J Mol Sci.* (2020) 21:9372. doi: 10.3390/ijms21249372

7. Takata F, Nakagawa S, Matsumoto J, Dohgu S. Blood-brain barrier dysfunction amplifies the development of neuroinflammation: understanding of cellular events in brain microvascular endothelial cells for prevention and treatment of BBB dysfunction. *Front Cell Neurosci.* (2021) 15:661838. doi: 10.3389/fncel.2021.661838

8. Maron DJ. The epidemiology of low levels of high-density lipoprotein cholesterol in patients with and without coronary artery disease. *Am J Cardiol.* (2000) 86:11L–14L. doi: 10.1016/S0002-9149(00)01462-4

9. Dullaart RP, Annema W, de Boer JF, Tietge UJ. Pancreatic beta-cell function relates positively to HDL functionality in well-controlled type 2 diabetes mellitus. *Atherosclerosis.* (2012) 222:567–73. doi: 10.1016/j.atherosclerosis.2012.03.037

10. Mulder DJ, de Boer JF, Graaff R, de Vries R, Annema W, Lefrandt JD, et al. Skin autofluorescence is inversely related to HDL anti-oxidative capacity in type 2 diabetes mellitus. *Atherosclerosis.* (2011) 218:102–6. doi: 10.1016/j.atherosclerosis.2011.05.011

11. Scheffer PG, Tushuizen ME, Vermue HP, Schindhelm RK, Rustemeijer C, Diamant M. Effect of three consecutive meals on the physicochemical properties of HDL and LDL in individuals with the metabolic syndrome and patients with type 2 diabetes. *Eur J Clin Nutr.* (2011) 65:1242–9. doi: 10.1038/ejcn.2011.114

12. Kruit JK, Brunham LR, Verchere CB, Hayden MR. HDL and LDL cholesterol significantly influence beta-cell function in type 2 diabetes mellitus. *Curr Opin Lipidol.* (2010) 21:178–85. doi: 10.1097/MOL.0b013e328339387b

13. Ye X, Chopp M, Liu X, Zacharek A, Cui X, Yan T, et al. Niaspan reduces high-mobility group box 1/receptor for advanced glycation endproducts after stroke in type-1 diabetic rats. *Neuroscience.* (2011) 190:339–45. doi: 10.1016/j.neuroscience.2011.06.004

14. Williams MD, Nadler JL. Inflammatory mechanisms of diabetic complications. *Curr Diab Rep.* (2007) 7:242–8. doi: 10.1007/s11892-007-0038-y

15. Cui X, Chopp M, Zacharek A, Roberts C, Buller B, Ion M, et al. Niacin treatment of stroke increases synaptic plasticity and axon growth in rats. *Stroke.* (2010) 41:2044–9. doi: 10.1161/STROKEAHA.110.589333

16. Cui X, Chopp M, Zacharek A, Cui Y, Roberts C, Chen J. The neurorestorative benefit of gw3965 treatment of stroke in mice. *Stroke.* (2013) 44:153–61. doi: 10.1161/STROKEAHA.112.677682

17. Cui X, Chopp M, Zhang Z, Li R, Zacharek A, Landschoot-Ward J, et al. ABCA1/ApoE/HDL pathway mediates GW3965-induced neurorestoration after stroke. *Stroke.* (2017) 48:459–67. doi: 10.1161/STROKEAHA.116.015592

18. Cui X, Chopp M, Zacharek A, Cui C, Yan T, Ning R, et al. D-4F decreases white matter damage after stroke in mice. *Stroke.* (2016) 47:214–20. doi: 10.1161/STROKEAHA.115.011046

19. Chen J, Cui X, Zacharek A, Jiang H, Roberts C, Zhang C, et al. Niaspan increases angiogenesis and improves functional recovery after stroke. *Ann Neurol.* (2007) 62:49–58. doi: 10.1002/ana.21160

20. Sfredel V, Mota M, Iancu I, Danoiu S, Mitran SI, Balseanu AT, et al. Correlations between abdominal circumference and the breakage resistance of the fibrin clot in patients with diabetes mellitus type 2. *Rom J Intern Med.* (2010) 48:165–71.

21. Gotto AM Jr, Brinton EA. Assessing low levels of high-density lipoprotein cholesterol as a risk factor in coronary heart disease: a working group report and update. *J Am Coll Cardiol.* (2004) 43:717–24. doi: 10.1016/j.jacc.2003.08.061

22. Sharrett AR, Ballantyne CM, Coady SA, Heiss G, Sorlie PD, Catellier D, et al. Coronary heart disease prediction from lipoprotein cholesterol levels, triglycerides, lipoprotein(a), apolipoproteins A-I and B, and HDL density subfractions: the atherosclerosis risk in communities (ARIC) study. *Circulation.* (2001) 104:1108–13. doi: 10.1161/hc3501.095214

23. Bonora E. The metabolic syndrome and cardiovascular disease. *Ann Med.* (2006) 38:64–80. doi: 10.1080/07853890500401234

24. Anan F, Masaki T, Kikuchi H, Iwao T, Shimomura T, Umeno Y, et al. Association between plasma high-sensitivity c-reactive protein and insulin resistance and white matter lesions in Japanese type 2 diabetic patients. *Diabetes Res Clin Pract.* (2010) 87:233–9. doi: 10.1016/j.diabres.2009.10.017

25. Kontush A, Chapman MJ. Functionally defective high-density lipoprotein: a new therapeutic target at the crossroads of dyslipidemia, inflammation, and atherosclerosis. *Pharmacol Rev.* (2006) 58:342–74. doi: 10.1124/pr.58.3.1

26. Vance JE, Hayashi H. Formation and function of apolipoprotein E-containing lipoproteins in the nervous system. *Biochim Biophys Acta.* (2010) 1801:806–18. doi: 10.1016/j.bbalip.2010.02.007

27. Stukas S, May S, Wilkinson A, Chan J, Donkin J, Wellington CL. The LXR agonist GW3965 increases apoA-I protein levels in the central nervous system independent of ABCA1. *Biochim Biophys Acta.* (2012) 1821:536–46. doi: 10.1016/j.bbalip.2011.08.014

28. Brunham LR, Singaraja RR, Duong M, Timmins JM, Fievet C, Bissada N, et al. Tissue-specific roles of abca1 influence susceptibility to atherosclerosis. *Arterioscler Thromb Vasc Biol.* (2009) 29:548–54. doi: 10.1161/ATVBAHA.108.182303

29. Karasinska JM, de Haan W, Franciosi S, Ruddle P, Fan J, Kruit JK, et al. Abca1 influences neuroinflammation and neuronal death. *Neurobiol Dis.* (2013) 54:445–55. doi: 10.1016/j.nbd.2013.01.018

30. Khalil A, Berrougui H, Pawelec G, Fulop T. Impairment of the ABCA1 and SR-BI-mediated cholesterol efflux pathways and HDL anti-inflammatory activity in Alzheimer's disease. *Mech Ageing Dev.* (2012) 133:20–9. doi: 10.1016/j.mad.2011.11.008

31. Moore RE, Navab M, Millar JS, Zimetti F, Hama S, Rothblat GH, et al. Increased atherosclerosis in mice lacking apolipoprotein A-I attributable to both impaired reverse cholesterol transport and increased inflammation. *Circ Res.* (2005) 97:763–71. doi: 10.1161/01.RES.0000185320.82962.F7

32. Shao B. Site-specific oxidation of apolipoprotein A-I impairs cholesterol export by ABCA1, a key cardioprotective function of HDL. *Biochim Biophys Acta.* (2012) 1821:490–501. doi: 10.1016/j.bbalip.2011.11.011

33. Tang C, Liu Y, Kessler PS, Vaughan AM, Oram JF. The macrophage cholesterol exporter abca1 functions as an anti-inflammatory receptor. *J Biol Chem.* (2009) 284:32336–43. doi: 10.1074/jbc.M109.047472

34. Cui X, Chopp M, Zacharek A, Karasinska JM, Cui Y, Ning R, et al. Deficiency of brain ATP-binding cassette transporter a-1 exacerbates blood-brain barrier and white matter damage after stroke. *Stroke.* (2015) 46:827–34. doi: 10.1161/STROKEAHA.114.007145

35. Wang X, Li R, Zacharek A, Landschoot-Ward J, Wang F, Wu KH, et al. Administration of downstream ApoE attenuates the adverse effect of brain ABCA1 deficiency on stroke. *Int J Mol Sci.* (2018) 19:3368. doi: 10.3390/ijms19113368

36. Li L, Li R, Zacharek A, Wang F, Landschoot-Ward J, Chopp M, et al. ABCA1/ApoE/HDL signaling pathway facilitates myelination and oligodendrogenesis after stroke. *Int J Mol Sci.* (2020) 21:4369. doi: 10.3390/ijms21124369

37. Sherman CB, Peterson SJ, Frishman WH. Apolipoprotein A-I mimetic peptides: a potential new therapy for the prevention of atherosclerosis. *Cardiol Rev.* (2010) 18:141–7. doi: 10.1097/CRD.0b013e3181c4b508

38. Navab M, Anantharamaiah GM, Reddy ST, Hama S, Hough G, Grijalva VR, et al. Oral D-4F causes formation of pre-beta high-density lipoprotein and improves high-density lipoprotein-mediated cholesterol efflux and reverse cholesterol transport from macrophages in apolipoprotein E-null mice. *Circulation.* (2004) 109:3215–20. doi: 10.1161/01.CIR.0000134275.90823.87

39. Chen X, Burton C, Song X, McNamara L, Langella A, Cianetti S, et al. An apoA-I mimetic peptide increases LCAT activity in mice through increasing HDL concentration. *Int J Biol Sci.* (2009) 5:489–99. doi: 10.7150/ijbs.5.489

40. Song X, Fischer P, Chen X, Burton C, Wang J. An apoA-I mimetic peptide facilitates off-loading cholesterol from HDL to liver cells through scavenger receptor BI. *Int J Biol Sci.* (2009) 5:637–46. doi: 10.7150/ijbs.5.637

41. Xie Q, Zhao S. Effect of apolipoprotein A-I mimetic peptides on cholesterol efflux in RAW264.7 cells. *J Central South Univ.* (2011) 36:51–7. doi: 10.3969/j.issn.1672-7347.2011.01.008

42. Xie Q, Zhao SP, Li F. D-4f, an apolipoprotein A-I mimetic peptide, promotes cholesterol efflux from macrophages via ATP-binding cassette transporter A1. *Tohoku J Exp Med.* (2010) 220:223–8. doi: 10.1620/tjem.220.223

43. Ying R, Yuan Y, Qin YF, Tian D, Feng L, Guo ZG, et al. The combination of l-4F and simvastatin stimulate cholesterol efflux and related proteins expressions to reduce atherosclerotic lesions in apoE knockout mice. *Lipids Health Dis.* (2013) 12:180. doi: 10.1186/1476-511X-12-180

44. Navab M, Anantharamaiah GM, Reddy ST, Van Lenten BJ, Wagner AC, Hama S, et al. An oral apoJ peptide renders HDL antiinflammatory in mice and monkeys and dramatically reduces atherosclerosis in apolipoprotein E-null mice. *Arterioscler Thromb Vasc Biol.* (2005) 25:1932–7. doi: 10.1161/01.ATV.0000174589.70190.e2

45. Ning R, Venkat P, Chopp M, Zacharek A, Yan T, Cui X, et al. D-4F increases microRNA-124a and reduces neuroinflammation in diabetic stroke rats. *Oncotarget.* (2017) 8:95481–94. doi: 10.18632/oncotarget.20751

46. Wang X, Li R, Zacharek A, Landschoot-Ward J, Chopp M, Chen J, et al. Apoa-i mimetic peptide reduces vascular and white matter damage after stroke in type-2 diabetic mice. *Front Neurosci.* (2019) 13:1127. doi: 10.3389/fnins.2019.01127

47. Karasinska JM, Rinninger F, Lutjohann D, Ruddle P, Franciosi S, Kruit JK, et al. Specific loss of brain abca1 increases brain cholesterol uptake and influences neuronal structure and function. *J Neurosci.* (2009) 29:3579–3589. doi: 10.1523/JNEUROSCI.4741-08.2009

48. Ding G, Chen J, Chopp M, Li L, Yan T, Li Q, et al. Cell treatment for stroke in type two diabetic rats improves vascular permeability measured by MRI. *PLoS ONE.* (2016) 11:e0149147. doi: 10.1371/journal.pone.0149147

49. Yan T, Venkat P, Chopp M, Zacharek A, Ning R, Cui Y, et al. Neurorestorative therapy of stroke in type 2 diabetes mellitus rats treated with human umbilical cord blood cells. *Stroke.* (2015) 46:2599–606. doi: 10.1161/STROKEAHA.115.009870

50. Ding G, Yan T, Chen J, Chopp M, Li L, Li Q, et al. Persistent cerebrovascular damage after stroke in type two diabetic rats measured by magnetic resonance imaging. *Stroke.* (2015) 46:507–12. doi: 10.1161/STROKEAHA.114.007538

51. Ding G, Chen J, Chopp M, Li L, Yan T, Davoodi-Bojd E, et al. White matter changes after stroke in type 2 diabetic rats measured by diffusion magnetic resonance imaging. *J Cereb Blood Flow Metab.* (2017) 37:241–51. doi: 10.1177/0271678X15622464

52. Mali VR, Ning R, Chen J, Yang XP, Xu J, Palaniyandi SS. Impairment of aldehyde dehydrogenase-2 by 4-hydroxy-2-nonenal adduct formation and cardiomyocyte hypertrophy in mice fed a high-fat diet and injected with low-dose streptozotocin. *Exp Biol Med.* (2014) 239:610–8. doi: 10.1177/1535370213520109

53. Freret T, Bouet V, Leconte C, Roussel S, Chazalviel L, Divoux D, et al. Behavioral deficits after distal focal cerebral ischemia in mice: usefulness of adhesive removal test. *Behav Neurosci.* (2009) 123:224–30. doi: 10.1037/a0014157

54. Swanson RA, Morton MT, Tsao-Wu G, Savalos RA, Davidson C, Sharp FR. A semiautomated method for measuring brain infarct volume. *J Cereb Blood Flow Metab.* (1990) 10:290–3. doi: 10.1038/jcbfm.1990.47

55. Zhang RL, Chopp M, Roberts C, Wei M, Wang X, Liu X, et al. Sildenafil enhances neurogenesis and oligodendrogenesis in ischemic brain of middle-aged mouse. *PLoS ONE.* (2012) 7:e48141. doi: 10.1371/journal.pone.0048141

56. Van Lenten BJ, Wagner AC, Jung CL, Ruchala P, Waring AJ, Lehrer RI, et al. Anti-inflammatory apoA-I-mimetic peptides bind oxidized lipids with much higher affinity than human apoA-I. *J Lipid Res.* (2008) 49:2302–11. doi: 10.1194/jlr.M800075-JLR200

57. Liu J, Yao S, Wang S, Jiao P, Song G, Yu Y, et al. D-4f, an apolipoprotein a-i mimetic peptide, protects human umbilical vein endothelial cells from oxidized low-density lipoprotein-induced injury by preventing the downregulation of pigment epithelium-derived factor expression. *J Cardiovasc Pharmacol.* (2014) 63:553–61. doi: 10.1097/FJC.0000000000000080

58. Yao S, Tian H, Miao C, Zhang DW, Zhao L, Li Y, et al. D4F alleviates macrophage-derived foam cell apoptosis by inhibiting CD36 expression and ER stress-CHOP pathway. *J Lipid Res.* (2015) 56:836–47. doi: 10.1194/jlr.M055400

59. Ou J, Wang J, Xu H, Ou Z, Sorci-Thomas MG, Jones DW, et al. Effects of D-4F on vasodilation and vessel wall thickness in hypercholesterolemic LDL receptor-null and LDL receptor/apolipoprotein A-I double-knockout mice on western diet. *Circ Res.* (2005) 97:1190–7. doi: 10.1161/01.RES.0000190634.60042.cb

60. Yu R, Yekta B, Vakili L, Gharavi N, Navab M, Marelli D, et al. Proatherogenic high-density lipoprotein, vascular inflammation, and mimetic peptides. *Curr Atheroscler Rep.* (2008) 10:171–6. doi: 10.1007/s11883-008-0025-z

61. Navab M, Ruchala P, Waring AJ, Lehrer RI, Hama S, Hough G, et al. A novel method for oral delivery of apolipoprotein mimetic peptides synthesized from all L-amino acids. *J Lipid Res.* (2009) 50:1538–47. doi: 10.1194/jlr.M800539-JLR200

62. Nandedkar SD, Weihrauch D, Xu H, Shi Y, Feroah T, Hutchins W, et al. D-4F, an apoA-1 mimetic, decreases airway hyperresponsiveness, inflammation, and oxidative stress in a murine model of asthma. *J Lipid Res.* (2011) 52:499–508. doi: 10.1194/jlr.M012724

63. Qin S, Kamanna VS, Lai JH, Liu T, Ganji SH, Zhang L, et al. Reverse D4F, an apolipoprotein-AI mimetic peptide, inhibits atherosclerosis in ApoE-null mice. *J Cardiovasc Pharmacol Ther.* (2012) 17:334–43. doi: 10.1177/1074248411434598

64. Chen J, Cui X, Zacharek A, Cui Y, Roberts C, Chopp M. White matter damage and the effect of matrix metalloproteinases in type 2 diabetic mice after stroke. *Stroke.* (2011) 42:445–52. doi: 10.1161/STROKEAHA.110.596486

65. Tajes M, Ramos-Fernandez E, Weng-Jiang X, Bosch-Morato M, Guivernau B, Eraso-Pichot A, et al. The blood-brain barrier: structure, function and therapeutic approaches to cross it. *Mol Membr Biol.* (2014) 31:152–67. doi: 10.3109/09687688.2014.937468

66. Yamazaki Y, Baker DJ, Tachibana M, Liu CC, van Deursen JM, Brott TG, et al. Vascular cell senescence contributes to blood-brain barrier breakdown. *Stroke.* (2016) 47:1068–77. doi: 10.1161/STROKEAHA.115.010835

67. Ueno M. Molecular anatomy of the brain endothelial barrier: an overview of the distributional features. *Curr Med Chem.* (2007) 14:1199–206. doi: 10.2174/092986707780597943

68. Anan F, Masaki T, Iwao T, Eto T, Shimomura T, Umeno Y, et al. The role of microalbuminuria and insulin resistance as significant risk factors for white matter lesions in japanese type 2 diabetic patients. *Curr Med Res Opin.* (2008) 24:1561–7. doi: 10.1185/03007990802061818

69. Hu J, Liu B, Zhao Q, Jin P, Hua F, Zhang Z, et al. Bone marrow stromal cells inhibits hmgb1-mediated inflammation after stroke in type 2 diabetic rats. *Neuroscience.* (2016) 324:11–9. doi: 10.1016/j.neuroscience.2016.02.058

70. Ma S, Wang J, Wang Y, Dai X, Xu F, Gao X, et al. Diabetes mellitus impairs white matter repair and long-term functional deficits after cerebral ischemia. *Stroke.* (2018) 49:2453–63. doi: 10.1161/STROKEAHA.118.021452

71. Yan T, Venkat P, Chopp M, Zacharek A, Ning R, Roberts C, et al. Neurorestorative responses to delayed human mesenchymal stromal cells treatment of stroke in type 2 diabetic rats. *Stroke.* (2016) 47:2850–8. doi: 10.1161/STROKEAHA.116.014686

72. Pikula A, Howard BV, Seshadri S. Stroke and diabetes. In: Cowie CC, Casagrande SS, Menke A, Cissell MA, Eberhardt MS, et al., editors. *Diabetes in America.* Bethesda, MD: National Institute of Diabetes and Digestive and Kidney Diseases (2018).

73. Yatomi Y, Tanaka R, Shimada Y, Yamashiro K, Liu M, Mitome-Mishima Y, et al. Type 2 diabetes reduces the proliferation and survival of oligodendrocyte progenitor cells in ishchemic white matter lesions. *Neuroscience.* (2015) 289:214–23. doi: 10.1016/j.neuroscience.2014.12.054

74. Rosenbaum MA, Chaudhuri P, Abelson B, Cross BN, Graham LM. Apolipoprotein a-i mimetic peptide reverses impaired arterial healing after injury by reducing oxidative stress. *Atherosclerosis.* (2015) 241:709–15. doi: 10.1016/j.atherosclerosis.2015.06.018

75. Woo JM, Lin Z, Navab M, Van Dyck C, Trejo-Lopez Y, Woo KM, et al. Treatment with apolipoprotein a-1 mimetic peptide reduces lupus-like manifestations in a murine lupus model of accelerated atherosclerosis. *Arthr Res Ther.* (2010) 12:R93. doi: 10.1186/ar3020

76. Diditchenko S, Gille A, Pragst I, Stadler D, Waelchli M, Hamilton R, et al. Novel formulation of a reconstituted high-density lipoprotein (csl112) dramatically enhances abca1-dependent cholesterol efflux. *Arterioscler Thromb Vasc Biol.* (2013) 33:2202–11. doi: 10.1161/ATVBAHA.113.301981

77. Duong PT, Collins HL, Nickel M, Lund-Katz S, Rothblat GH, Phillips MC. Characterization of nascent HDL particles and microparticles formed by ABCA1-mediated efflux of cellular lipids to apoA-I. *J Lipid Res.* (2006) 47:832–43. doi: 10.1194/jlr.M500531-JLR200

78. Getz GS, Wool GD, Reardon CA. HDL apolipoprotein-related peptides in the treatment of atherosclerosis and other inflammatory disorders. *Curr Pharm Des.* (2010) 16:3173–84. doi: 10.2174/138161210793292492

79. Shao B, Heinecke JW. Impact of hdl oxidation by the myeloperoxidase system on sterol efflux by the abca1 pathway. *J Proteom.* (2011) 74:2289–99. doi: 10.1016/j.jprot.2011.04.001

80. Yin K, Chen WJ, Zhou ZG, Zhao GJ, Lv YC, Ouyang XP, et al. Apolipoprotein A-I inhibits CD40 proinflammatory signaling via ATP-binding cassette transporter a1-mediated modulation of lipid raft in macrophages. *J Atheroscler Thromb.* (2012) 19:823–36. doi: 10.5551/jat.12823

81. Ballerini P, Ciccarelli R, Di Iorio P, Buccella S, D'Alimonte I, Giuliani P, et al. Guanosine effect on cholesterol efflux and apolipoprotein E expression in astrocytes. *Purinergic Signal.* (2006) 2:637–49. doi: 10.1007/s11302-006-9011-5

82. Lund-Katz S, Phillips MC. High density lipoprotein structure-function and role in reverse cholesterol transport. *Subcell Biochem.* (2010) 51:183–227. doi: 10.1007/978-90-481-8622-8_7

83. Hirsch-Reinshagen V, Zhou S, Burgess BL, Bernier L, McIsaac SA, Chan JY, et al. Deficiency of abca1 impairs apolipoprotein e metabolism in brain. *J Biol Chem.* (2004) 279:41197–207. doi: 10.1074/jbc.M407962200

84. Koldamova RP, Lefterov IM, Ikonomovic MD, Skoko J, Lefterov PI, Isanski BA, et al. 22r-hydroxycholesterol and 9-cis-retinoic acid induce atp-binding cassette transporter a1 expression and cholesterol efflux in brain cells and decrease amyloid beta secretion. *J Biol Chem.* (2003) 278:13244–56. doi: 10.1074/jbc.M300044200

85. Chen J, Zhang X, Kusumo H, Costa LG, Guizzetti M. Cholesterol efflux is differentially regulated in neurons and astrocytes: implications for brain cholesterol homeostasis. *Biochim Biophys Acta.* (2013) 1831:263–75. doi: 10.1016/j.bbalip.2012.09.007

86. Wahrle SE, Jiang H, Parsadanian M, Legleiter J, Han X, Fryer JD, et al. ABCA1 is required for normal central nervous system ApoE levels and for lipidation of astrocyte-secreted apoE. *J Biol Chem.* (2004) 279:40987–93. doi: 10.1074/jbc.M407963200

87. Kim WS, Guillemin GJ, Glaros EN, Lim CK, Garner B. Quantitation of atp-binding cassette subfamily-a transporter gene expression in primary human brain cells. *Neuroreport.* (2006) 17:891–6. doi: 10.1097/01.wnr.0000221833.41340.cd

88. Navab M, Anantharamaiah GM, Reddy ST, Hama S, Hough G, Grijalva VR, et al. Apolipoprotein A-I mimetic peptides. *Arterioscler Thromb Vasc Biol.* (2005) 25:1325–31. doi: 10.1161/01.ATV.0000165694.39518.95

89. Navab M, Anantharamaiah GM, Hama S, Hough G, Reddy ST, Frank JS, et al. D-4F and statins synergize to render HDL antiinflammatory in mice and monkeys and cause lesion regression in old apolipoprotein E-null mice. *Arterioscler Thromb Vasc Biol.* (2005) 25:1426–32. doi: 10.1161/01.ATV.0000167412.98221.1a

90. Vaziri ND, Kim HJ, Moradi H, Farmand F, Navab K, Navab M, et al. Amelioration of nephropathy with apoA-1 mimetic peptide in apoE-deficient mice. *Nephrol Dial Transplant.* (2010) 25:3525–34. doi: 10.1093/ndt/gfq274

91. Navab M, Anantharamaiah GM, Reddy ST, Van Lenten BJ, Datta G, Garber D, et al. Potential clinical utility of high-density lipoprotein-mimetic peptides. *Curr Opin Lipidol.* (2006) 17:440–4. doi: 10.1097/01.mol.0000236371.27508.d4

92. Tsuchida Y, Zhong J, Otsuka T, Dikalova A, Pastan I, Anantharamaiah GM, et al. Lipoprotein modulation of proteinuric renal injury. *Lab Invest.* (2019) 99:1107–16. doi: 10.1038/s41374-019-0253-6

93. Kruger AL, Peterson S, Turkseven S, Kaminski PM, Zhang FF, Quan S, et al. D-4F induces heme oxygenase-1 and extracellular superoxide dismutase, decreases endothelial cell sloughing, and improves vascular reactivity in rat model of diabetes. *Circulation.* (2005) 111:3126–34. doi: 10.1161/CIRCULATIONAHA.104.517102

94. Ennis SR, Keep RF. Effect of sustained-mild and transient-severe hyperglycemia on ischemia-induced blood-brain barrier opening. *J Cereb Blood Flow Metab.* (2007) 27:1573–82. doi: 10.1038/sj.jcbfm.9600454

95. Ergul A, Elgebaly MM, Middlemore ML, Li W, Elewa H, Switzer JA, et al. Increased hemorrhagic transformation and altered infarct size and localization after experimental stroke in a rat model type 2 diabetes. *BMC Neurol.* (2007) 7:33. doi: 10.1186/1471-2377-7-33

96. Peterson SJ, Husney D, Kruger AL, Olszanecki R, Ricci F, Rodella LF, et al. Long-term treatment with the apolipoprotein a1 mimetic peptide increases antioxidants and vascular repair in type i diabetic rats. *J Pharmacol Exp Ther.* (2007) 322:514–20. doi: 10.1124/jpet.107.119479

97. Cui X, Chopp M, Zacharek A, Ye X, Roberts C, Chen J. Angiopoietin/tie2 pathway mediates type 2 diabetes induced vascular damage after cerebral stroke. *Neurobiol Dis.* (2011) 43:285–92. doi: 10.1016/j.nbd.2011.04.005

98. Dunbar RL, Movva R, Bloedon LT, Duffy D, Norris RB, Navab M, et al. Oral apolipoprotein A-I mimetic D-4F lowers hdl-inflammatory index in high-risk patients: a first-in-human multiple-dose, randomized controlled trial. *Clin Transl Sci.* (2017) 10:455–69. doi: 10.1111/cts.12487

99. Li R, Navab M, Pakbin P, Ning Z, Navab K, Hough G, et al. Ambient ultrafine particles alter lipid metabolism and HDL anti-oxidant capacity in LDLR-null mice. *J Lipid Res.* (2013) 54:1608–15. doi: 10.1194/jlr.M035014

100. Bloedon LT, Dunbar R, Duffy D, Pinell-Salles P, Norris R, DeGroot BJ, et al. Safety, pharmacokinetics, and pharmacodynamics of oral apoA-I mimetic peptide D-4F in high-risk cardiovascular patients. *J Lipid Res.* (2008) 49:1344–52. doi: 10.1194/jlr.P800003-JLR200

101. Morgantini C, Imaizumi S, Grijalva V, Navab M, Fogelman AM, Reddy ST. Apolipoprotein A-I mimetic peptides prevent atherosclerosis development and reduce plaque inflammation in a murine model of diabetes. *Diabetes.* (2010) 59:3223–8. doi: 10.2337/db10-0844

102. Navab M, Anantharamaiah GM, Reddy ST, Fogelman AM. Apolipoprotein A-I mimetic peptides and their role in atherosclerosis prevention. *Nat Clin Pract.* (2006) 3:540–7. doi: 10.1038/ncpcardio0661

103. Navab M, Anantharamaiah GM, Hama S, Garber DW, Chaddha M, Hough G, et al. Oral administration of an Apo A-I mimetic peptide synthesized from d-amino acids dramatically reduces atherosclerosis in mice independent of plasma cholesterol. *Circulation.* (2002) 105:290–2. doi: 10.1161/hc0302.103711

104. Navab M, Anantharamaiah GM, Reddy ST, Van Lenten BJ, Datta G, Garber D, et al. Human apolipoprotein A-I and A-I mimetic peptides: Potential for atherosclerosis reversal. *Curr Opin Lipidol.* (2004) 15:645–9. doi: 10.1097/00041433-200412000-00004

105. Meyer P, Nigam A, Marcil M, Tardif JC. The therapeutic potential of high-density lipoprotein mimetic agents in coronary artery disease. *Curr Atheroscler Rep.* (2009) 11:329–33. doi: 10.1007/s11883-009-0049-z

106. McGrath KC, Li X, Twigg SM, Heather AK. Apolipoprotein-ai mimetic peptides d-4f and l-5f decrease hepatic inflammation and increase insulin sensitivity in c57bl/6 mice. *PLoS ONE.* (2020) 15:e0226931. doi: 10.1371/journal.pone.0226931

107. Xu W, Qian M, Huang C, Cui P, Li W, Du Q, et al. Comparison of mechanisms of endothelial cell protections between high-density lipoprotein and apolipoprotein A-I mimetic peptide. *Front Pharmacol.* (2019) 10:817. doi: 10.3389/fphar.2019.00817

108. Mineo C, Shaul PW. Regulation of signal transduction by HDL. *J Lipid Res.* (2013) 54:2315–24. doi: 10.1194/jlr.R039479

109. Ou J, Ou Z, Jones DW, Holzhauer S, Hatoum OA, Ackerman AW, et al. L-4F, an apolipoprotein a-1 mimetic, dramatically improves vasodilation in hypercholesterolemia and sickle cell disease. *Circulation.* (2003) 107:2337–41. doi: 10.1161/01.CIR.0000070589.61860.A9

110. Meriwether D, Imaizumi S, Grijalva V, Hough G, Vakili L, Anantharamaiah GM, et al. Enhancement by LDL of transfer of l-4F and oxidized lipids to HDL in C57BL/6J mice and human plasma. *J Lipid Res.* (2011) 52:1795–809. doi: 10.1194/jlr.M016741

111. Umar S, Ruffenach G, Moazeni S, Vaillancourt M, Hong J, Cunningham C, et al. Involvement of low-density lipoprotein receptor in the pathogenesis of pulmonary hypertension. *J Am Heart Assoc.* (2020) 9:e012063. doi: 10.1161/JAHA.119.012063

112. Kelesidis T, Yang OO, Currier JS, Navab K, Fogelman AM, Navab M. HIV-1 infected patients with suppressed plasma viremia on treatment have pro-inflammatory HDL. *Lipids Health Dis.* (2011) 10:35. doi: 10.1186/1476-511X-10-35

113. Song X, Shi Y, You J, Wang Z, Xie L, Zhang C, et al. D-4F, an apolipoprotein A-I mimetic, suppresses IL-4 induced macrophage alternative activation and pro-fibrotic TGF-beta1 expression. *Pharm Biol.* (2019) 57:470–476. doi: 10.1080/13880209.2019.1640747

114. Gupta H, Dai L, Datta G, Garber DW, Grenett H, Li Y, et al. Inhibition of lipopolysaccharide-induced inflammatory responses by an apolipoprotein AI mimetic peptide. *Circ Res.* (2005) 97:236–43. doi: 10.1161/01.RES.0000176530.66400.48

115. Yang N, Tian H, Zhan E, Zhai L, Jiao P, Yao S, et al. Reverse-D-4F improves endothelial progenitor cell function and attenuates LPS-induced acute lung injury. *Respir Res.* (2019) 20:131. doi: 10.1186/s12931-019-1099-6

116. Van Lenten BJ, Wagner AC, Navab M, Anantharamaiah GM, Hama S, Reddy ST, et al. Lipoprotein inflammatory properties and serum amyloid a levels but not cholesterol levels predict lesion area in cholesterol-fed rabbits. *J Lipid Res.* (2007) 48:2344–53. doi: 10.1194/jlr.M700138-JLR200

117. Van Lenten BJ, Wagner AC, Anantharamaiah GM, Garber DW, Fishbein MC, Adhikary L, et al. Influenza infection promotes macrophage traffic into arteries of mice that is prevented by D-4F, an apolipoprotein A-I mimetic peptide. *Circulation.* (2002) 106:1127–32. doi: 10.1161/01.CIR.0000030182.35880.3E

118. Lin S, Fan LW, Pang Y, Rhodes PG, Mitchell HJ, Cai Z. IGF-1 protects oligodendrocyte progenitor cells and improves neurological functions following cerebral hypoxia-ischemia in the neonatal rat. *Brain Res.* (2005) 1063:15–26. doi: 10.1016/j.brainres.2005.09.042

119. Bake S, Selvamani A, Cherry J, Sohrabji F. Blood brain barrier and neuroinflammation are critical targets of IGF-1-mediated neuroprotection in stroke for middle-aged female rats. *PLoS ONE.* (2014) 9:e91427. doi: 10.1371/journal.pone.0091427

120. Tang SL, Chen WJ, Yin K, Zhao GJ, Mo ZC, Lv YC, et al. Papp-a negatively regulates ABCA1, ABCG1 and SR-B1 expression by inhibiting LXRalpha through the IGF-I-mediated signaling pathway. *Atherosclerosis.* (2012) 222:344–54. doi: 10.1016/j.atherosclerosis.2012.03.005

121. Morgantini C, Natali A, Boldrini B, Imaizumi S, Navab M, Fogelman AM, et al. Anti-inflammatory and antioxidant properties of HDLs are impaired in type 2 diabetes. *Diabetes.* (2011) 60:2617–23. doi: 10.2337/db11-0378